. .

The HERMES Experiment

Stephen F. Pate
Physics Department, New Mexico State University, Las Cruces NM 88003
(for the HERMES Collaboration)

(1) Introduction: Overview of Deep Inelastic Scattering and the Spin Structure of the Nucleon

(2) Apparatus: How the HERMES Experiment works

(3) Results I: The Gottfried Sum Rule and the Light Quark Sea Flavor Asymmetry

(4) Results II: The Polarized Quark Distributions of the Nucleon

(5) Results III: Polarization of Λ's produced in Deep Inelastic Scattering

[Presentation at HUGS 1999, Jefferson Lab, Newport News, VA.]

Deep Inelastic Scattering

Deep inelastic scattering occurs when a high energy lepton interacts with an individual quark inside of a nucleon or nucleus, with sufficient momentum transfer (more than 1 GeV/c) such that the interaction can be treated in an impulse approximation. Deep inelastic scattering has been the fundamental experimental probe of the internal structure of the nucleon for the past three decades.

The incident lepton, of energy E, interacts with a quark of flavor f (up, down, strange...) *via* a virtual photon of energy ν and momentum $\vec{q}$, so that the scattered lepton has remaining energy $E' = E - \nu$. The positive square of the four–momentum transfer q of the virtual photon, denoted by $Q^2 = -q^2$, and the Bjorken momentum fraction of the struck quark, $x = Q^2/2M\nu$, are used to characterize the kinematics of the deep inelastic scattering process. (M is the mass of the nucleon.)

Deep inelastic scattering of leptons from nucleons probes the quark distribution functions:

- $q_f^+(x, Q^2)$ probability of finding a quark of flavor f and Bjorken momentum fraction x with helicity parallel (+) to the nucleon spin, at a given momentum transfer Q^2
- $q_f(x, Q^2) = q_f^+(x, Q^2) + q_f^-(x, Q^2)$ **unpolarized distribution functions**
- $\Delta q_f(x, Q^2) = q_f^+(x, Q^2) - q_f^-(x, Q^2)$ **polarized distribution functions**

Kinematics of Deep Inelastic Scattering

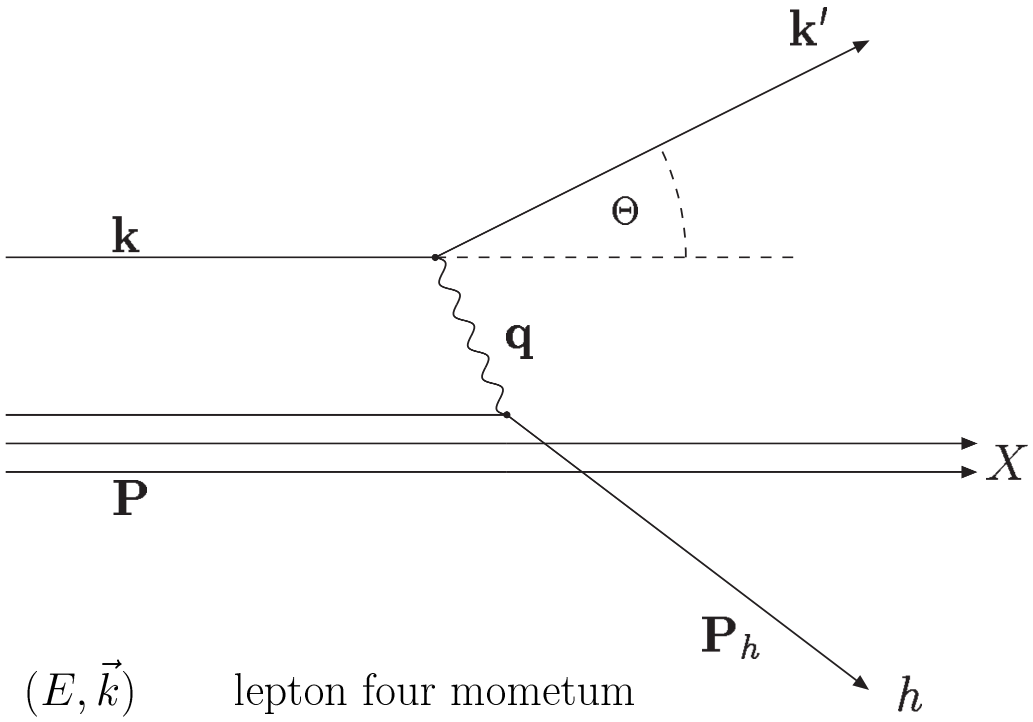

$$\mathbf{k} = (E, \vec{k}) \qquad \text{lepton four mometum}$$

$$\begin{aligned}\mathbf{q}^2 &= (\mathbf{k} - \mathbf{k}')^2 \qquad \text{mometum transfer} \\ &= 2m^2 + 2(kk'\cos\Theta - EE')\end{aligned}$$

$$\begin{aligned}Q^2 &= -\mathbf{q}^2 \\ &= 2EE'(\cos\Theta - 1) \qquad \text{Relativisic limit}: \quad m << E, \quad E \approx k \\ &= 4EE'\sin^2(\Theta/2)\end{aligned}$$

$$\nu = E - E' \qquad \text{virtual photon energy}$$

$$W^2 = (\mathbf{P} + \mathbf{q})^2 \qquad \text{photon} - \text{nucleon invariant mass}$$

$$x = Q^2/2M\nu \quad \text{parton momentum fraction;} \quad x_{\text{Bjorken}}$$

$$y = \nu/E \qquad \text{virtual photon energy fraction}$$

$$z = E_h/\nu \qquad \text{individual hadron energy fraction}$$

Inclusive Deep Inelastic Scattering

The cross section for *inclusive* deep inelastic scattering, in which only the scattered lepton is observed,

$$\frac{d^2\sigma}{dxdQ^2} = \frac{4\pi\alpha^2}{Q^4}\left[y^2 F_1(x,Q^2) + \frac{F_2(x,Q^2)}{x}\left(1 - y - \frac{Mxy}{2E}\right)\right]$$

measures the **unpolarized structure functions** F_1 and F_2. In the *quark-parton model*, these are

$$F_1(x) = \frac{1}{2}\sum_f e_f^2 q_f(x)$$

and

$$F_2(x) = 2xF_1(x) \quad (\mathrm{Callan-Gross\ relation})$$

These are now well measured.

If the lepton and nucleon are **longitudinally polarized**, then the **polarized structure function**

$$g_1(x) = \frac{1}{2}\sum_f e_f^2 \Delta q_f(x)$$

is obtained from the asymmetry in the yield of scattered leptons

$$\begin{aligned} A_{||}(x) &= \frac{\frac{d^2\sigma^-}{dxdQ^2} - \frac{d^2\sigma^+}{dxdQ^2}}{\frac{d^2\sigma^-}{dxdQ^2} + \frac{d^2\sigma^+}{dxdQ^2}} \\ &= \frac{N^-(x) - N^+(x)}{N^-(x) + N^+(x)}, \end{aligned}$$

where N is the normalized yield of leptons for beam and target helicities parallel (+) or antiparallel (−). This polarized structure function has only recently been well measured for the proton and neutron. The first good measurement, by the European Muon Collaboration, brought about the “nucleon spin crisis” which continues to be of interest today and is the motivation for the HERMES experiment.

Naive Quark Model for the Spin Structure of the Proton

The total spin of the nucleon is a sum of contributions from its constituents (quarks and gluons), and they can contribute though their own intrinsic spin and/or though orbital angular momentum:

$$S_z = \frac{1}{2} = \frac{1}{2}(\Delta u_v + \Delta d_v + \Delta q_s) + \Delta g + L_q + L_g$$

where Δu_v and Δd_v are the polarized valence u and d quark distribution functions, Δq_s represents the polarized quark distribution functions for all sea quarks, Δg is the polarized gluon distribution function, and L_q and L_g are the orbital angular momentum contributions from the quarks and gluons. The terms Δg, L_q, and L_g are not separately gauge invariant, but the sum $\Delta g + L_q + L_g$ is.

In the naive quark model we assume

- s-wave quark states
- sea-quarks unpolarized
- gluons unpolarized

and under those assumptions you can write down a fully antisymmetrized proton spin wavefunction;

$$\begin{aligned}|\Phi_p> \;=\; & \frac{1}{\sqrt{18}}|2u{\uparrow}u{\uparrow}d{\downarrow}+2d{\downarrow}u{\uparrow}u{\uparrow}+2u{\uparrow}d{\downarrow}u{\uparrow}-u{\downarrow}d{\uparrow}u{\uparrow}-u{\uparrow}u{\downarrow}d{\uparrow} \\ & -u{\downarrow}u{\uparrow}d{\uparrow}-d{\uparrow}u{\downarrow}u{\uparrow}-u{\uparrow}d{\uparrow}u{\downarrow}-d{\uparrow}u{\uparrow}u{\downarrow}>\end{aligned}$$

From this one can easily compute the moments Δu, Δd and Δs for the proton:

$$\begin{aligned}\Delta u &= <u{\uparrow}-u{\downarrow}> \\ &= \frac{1}{18}[+4\cdot 2+4\cdot 2+4\cdot 2-0-0-0-0-0-0] \\ &= +4/3 \\ \Delta d &= <d{\uparrow}-d{\downarrow}> \\ &= \frac{1}{18}[-4-4-4+1+1+1+1+1+1] \\ &= -1/3 \\ \Delta s &= 0\end{aligned}$$

The Ellis-Jaffe Sum Rule

The moments Δu, Δd, and Δs can be related to the measurement of the polarized structure function $g_1(x)$. As

$$
\begin{aligned}
g_1(x) &= \frac{1}{2}\sum_f e_f^2 \Delta q_f(x) \\
\text{then} & \\
g_1^p(x) &= \frac{1}{2}\left(\frac{4}{9}\Delta u(x) + \frac{1}{9}\Delta d(x) + \frac{1}{9}\Delta s(x) + \frac{4}{9}\Delta \bar{u}(x) + \frac{1}{9}\Delta \bar{d}(x) + \frac{1}{9}\Delta \bar{s}(x)\right) \\
\text{and} & \\
g_1^n(x) &= \frac{1}{2}\left(\frac{4}{9}\Delta d(x) + \frac{1}{9}\Delta u(x) + \frac{1}{9}\Delta s(x) + \frac{4}{9}\Delta \bar{d}(x) + \frac{1}{9}\Delta \bar{u}(x) + \frac{1}{9}\Delta \bar{s}(x)\right)
\end{aligned}
$$

where we have assumed isospin symmetry; thus $u_n(x) = d_p(x) \equiv d(x)$, and $u_p(x) = d_n(x) \equiv u(x)$. Then the moments are related to the integral of $g_1(x)$:

$$
\begin{aligned}
\Gamma_1^p &= \int_0^1 g_1^p(x)dx = \frac{1}{2}\left(\frac{4}{9}\Delta u + \frac{1}{9}\Delta d + \frac{1}{9}\Delta s\right) \\
\Gamma_1^n &= \int_0^1 g_1^p(x)dx = \frac{1}{2}\left(\frac{4}{9}\Delta d + \frac{1}{9}\Delta u + \frac{1}{9}\Delta s\right)
\end{aligned}
$$

where we adopt the convention that Δu (for example) sums over quark *and* anti-quark contributions, which inclusive deep-inelastic scattering cannot distinguish.

The integral of $g_1(x)$ can also be given in terms of the matrix elements of the quark SU(3) axial vector currents; a_0, a_3, and a_8:

$$
\Gamma_1 = \frac{1}{12}\left(a_3 + \frac{1}{\sqrt{3}}a_8 + \frac{4}{3}a_0\right),
$$

where

$$
\begin{aligned}
a_0 &= \Delta u + \Delta d + \Delta s \\
a_3 &= \Delta u - \Delta d \\
a_8 &= \frac{1}{\sqrt{3}}\left(\Delta u + \Delta d - 2\Delta s\right).
\end{aligned}
$$

The Ellis-Jaffe Sum Rule (more)

Values for a_3 and a_8 can be gotten from data on neutron and hyperon β-decay, as the same axial currents are involved:

$$\begin{aligned} a_3 &= D + F \\ a_8 &= \frac{1}{\sqrt{3}}(3F - D). \end{aligned}$$

where F and D are

$$\begin{aligned} F &= 0.477 \pm 0.012 \\ D &= 0.756 \pm 0.011 \end{aligned}$$

Combining this information with a measurement of $g_1(x)$ (for one of the proton or neutron) gives a_0 and thus the moments of the quark polarizations:

$$\begin{aligned} \Delta u &= \frac{1}{6}(2a_0 + 3a_3 + \sqrt{3}a_8) \\ \Delta d &= \frac{1}{6}(2a_0 - 3a_3 + \sqrt{3}a_8) \\ \Delta s &= \frac{1}{3}(a_0 - \sqrt{3}a_8) \end{aligned}$$

If one assumes $\Delta s = 0$ (as in the naive quark model), then one may calculate the first moments of the polarized structure function g_1 for the proton and the neutron from these basic QCD considerations. This result for the integrals $\int_0^1 g_1^p(x)dx$ and $\int_0^1 g_1^n(x)dx$ is called the Ellis-Jaffe sum rule:

$$\Gamma_1^p = \int_0^1 g_1^p(x)dx = 0.185$$

$$\Gamma_1^n = \int_0^1 g_1^n(x)dx = -0.024$$

A Crisis is Born

In the late 1980's, the European Muon Collaboration (EMC) measured $g_1^p(x)$ via an inclusive deep inelastic scattering of polarized muons from a polarized hydrogen target. In 1987 they reported a value for the $g_1^p(x)$ integral of

$$\Gamma_1^p = 0.126 \pm 0.010 \pm 0.015$$

considerably shy of the value of $\Gamma_1^p = \int_0^1 g_1^p(x)dx = 0.185$ from the Ellis-Jaffe result which assumed $\Delta s = 0$.

However, this result indicates not only that perhaps $\Delta s \neq 0$, but also (and more importantly!) that the contribution of the quarks alone is insufficient to account for the spin of the proton. Using more recent data for Γ_1^p, and combining with the data from β-decay, one may calculate the moments of the quark polarizations from experiment:

$$\begin{aligned}
\Delta u &= +0.79 \pm 0.04 \\
\Delta d &= -0.45 \pm 0.04 \\
\Delta s &= -0.16 \pm 0.04
\end{aligned}$$

Thus the quark contribution to the proton spin is

$$\Delta\Sigma = \Delta u + \Delta d + \Delta s \approx 0.18$$

a far cry from 1.0! This result is the source of the "nucleon spin crisis" which was the motivation for the HERMES experiment.

Semi-inclusive Deep Inelastic Scattering

The quark which is struck in a deeply inelastic process will fragment into one or more hadrons. The number of hadrons of type h (pion, kaon, lambda...) produced is

$$N^h(x,z) \propto \sum_f e_f^2 q_f(x) D_f^h(z),$$

where $D_f^h(z)$ is the fragmentation function, expressing the probability that a quark of flavor f will produce a hadron of type h with energy fraction $z = E^h/\nu$, the fraction of the virtual photon energy carried away by the hadron.

Factorization: In the expression for the hadron multiplicity $N^h(x,z)$, the factor associated with the hard scattering process $(q_f(x))$ and the factor associated with the subsequent fragmentation$(D_f^h(z))$ are independent of each other. This expresses the underlying assumption of the impulse approximation, namely that the fragmentation process is entirely separate from the hard scattering process. We call this separation "factorization."

The Leading Hadron: The hadron produced with the largest energy fraction z, the so–called "leading hadron," will most likely carry the struck quark. More detailed information about the quark distribution functions is made available by detecting the leading hadron in coincidence with the scattered lepton. In particular, by examining the spin–dependent asymmetry in the yields of hadrons produced in deep-inelastic processes, the individual polarized quark distribution functions can be extracted. A detailed knowledge of these functions is vital to a resolution of the "nucleon spin crisis."

This is the main thrust of the HERMES physics program!

“Deep Inelastic Scattering” – 85 Years Ago

In 1914 Franck and Hertz performed an experiment which is in many ways equivalent in conception to the deep inelastic scattering experiments of today – only the energies (and price!) were about 9 orders of magnitude lower, and the apparatus was truly of the “table-top” variety. Only the existence of the electron was known and it was suspected that the energies of the atom were quantized – the Bohr model had been proposed only one year earlier. The cathode, heated by the

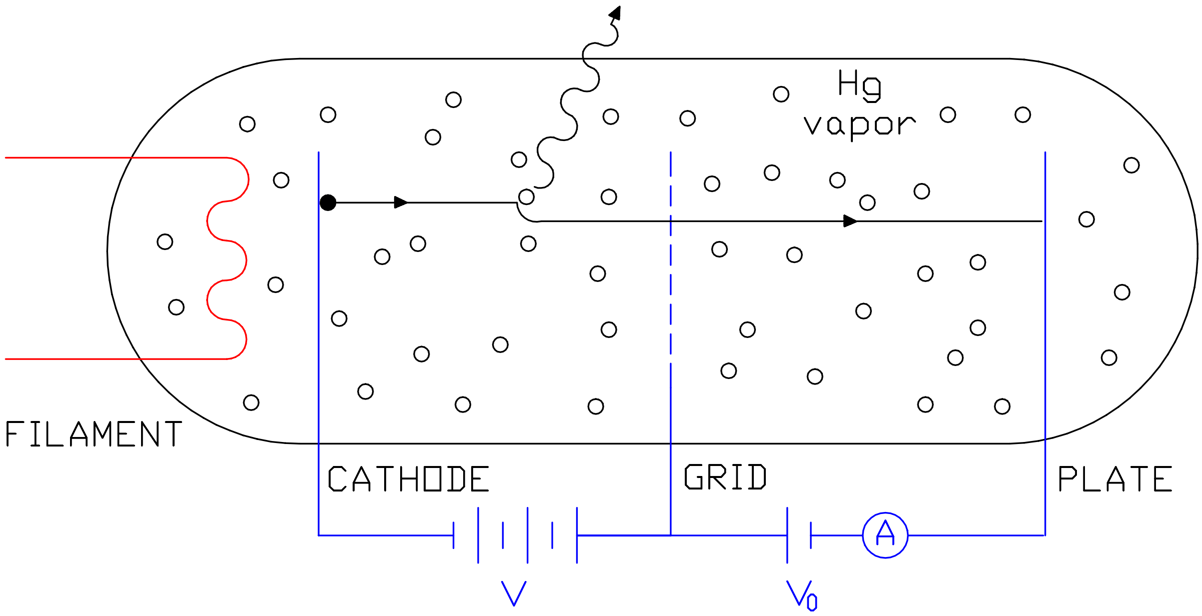

filament, emits electrons which are accelerated through the mercury vapor by the voltage V. A small retarding potential $V_0 << V$ between the grid and collecting plate is used to slow the electrons after they pass the grid.

If V is small, the electrons only recoil elastically from the atoms, and lose very little energy in doing so since the atoms weigh so much more. The electrons continue towards the plate and a current is seen in the ammeter A.

If V becomes large enough, the mercury atoms can be promoted to their first excited state and consequently the electron will lose that same amount of energy. Such electrons may lack suffient energy to pass from the grid to the plate. So it is observed that the plate current drops sharply when the voltage V is approximately equal to that of the first excitation energy of mercury, or multiples thereof. The emission of photons from the excited atoms is also observed.

The HERMES Experiment

HERMES is an internal target experiment located in the East Hall of the HERA storage ring complex at DESY. A beam of longitudinally polarized 27.5 GeV positrons in the HERA storage ring passes through the HERMES internal gas target. The target gases are polarized ^{3}He (1995), polarized ^{1}H (1996 and 1997), and various unpolarized gases (hydrogen, deuterium, ^{3}He, nitrogen) in all years. In 1998 and 1999 HERMES will employ a polarized ^{2}H target.

The HERMES spectrometer is constructed with an open geometry to allow detection of scattered leptons in coincidence with quark fragmentation products. Identification of detected particles is achieved through tracking, momentum reconstruction, and the differential responses of the various detector elements.

- typical HERA positron beam properties:
  energy = 27.5 GeV, current = 40 mA, lifetime = 10 h, polarization = 60%
- typical HERMES target properties:
  ^{3}He: thickness = 10^{15} nucleons/cm^2, polarization = 45%
  ^{1}H: thickness = 10^{14} nucleons/cm^2, polarization = 90%
  unpolarized gases: thickness in excess of 10^{15} nucleons/cm^2
- detector acceptance properties:
  angular range: $\pm$ (40 – 140) mrad vertical, $\pm$170 mrad horizontal
  Bjorken x: $0.021 < x < 0.85$
  momentum transfer: $0.8\ \mathrm{GeV}^2 < Q^2 < 20\ \mathrm{GeV}^2$, with $\langle Q^2 \rangle \approx 2.5\ \mathrm{GeV}^2$
  dipole field integral: 1.3 Tm
  tracking resolution: $\Delta p/p = 0.7$–1.3%, $\Delta\theta = 0.3$–0.6 mrad

HERMES Institutes

hermes
Knut Woller Nov 1998


University of Alberta
Argonne National Laboratory
INFN Bari
California Institute of Technology
University of Colorado
DESY Hamburg


DESY Zeuthen
JINR Dubna
Universität Erlangen-Nürnberg
Universita Ferrara
INFN Frascati
Universität Freiburg
Universiteit Gent

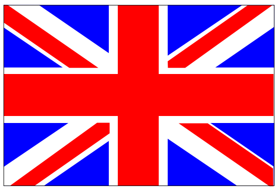
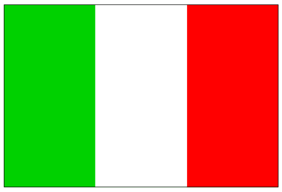

MPI Heidelberg
University of Illinois
University of Liverpool
University of Wisconsin-Madison
Massachusetts Institute of Technology
University of Michigan
LPI Moskau

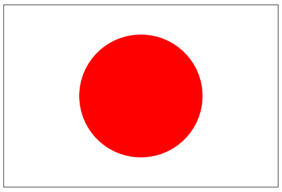
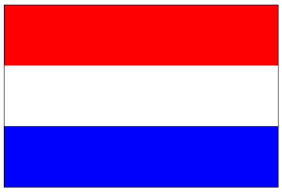

Universität München
New Mexico State University
NIKHEF Amsterdam
University of Pennsylvania
St. Petersburg NPI
INFN Roma
Simon Fraser University


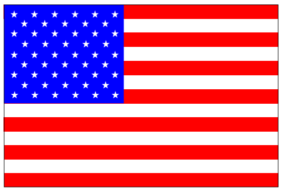

TRIUMF Vancouver
Tokyo Institute of Technology
Yerevan Physics Institute

Internal Gas Targets

The use of internal gas targets (10^{14} – 10^{15} nucleons/cm^2, a very low density compared to solid targets), in combination with a high intensity stored beam (10-40 mA), permits experiments to be done at useful luminosities of 10^{31} – 10^{32} cm^{-2}s^{-1} in a relatively background–free environment and a minimum of material between the detector and the event interaction point.

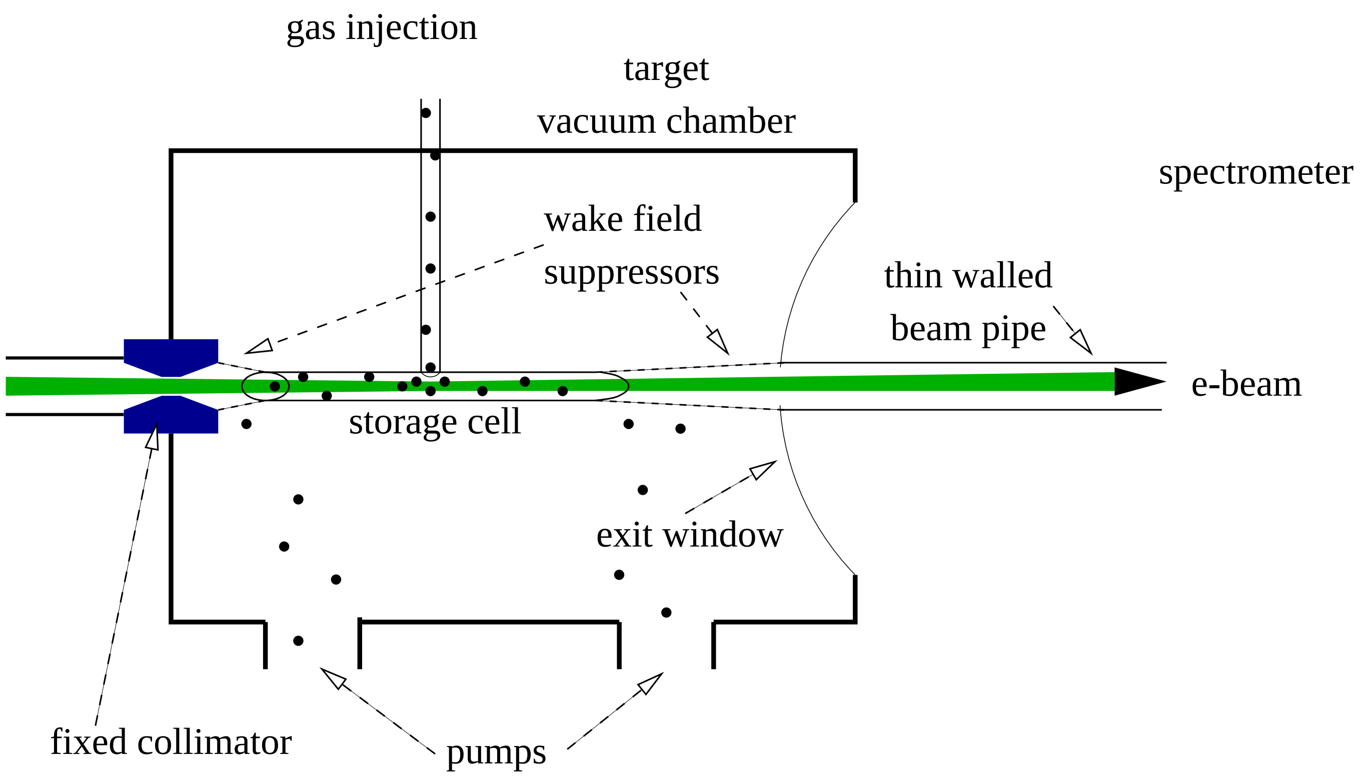

The storage cell is an elliptical cylinder, 400mm long, 29mm wide, and 9.8mm high, made from 125μm thick aluminum sheet. The collimator does not actually intercept the beam, but is in place to block the flux of synchrotron photons generated by the beam upstream of the target area. The dimensions of the cell and collimator are chosen so that the cell is not illuminated by any direct synchortron radiation – only radiation which has scattered at least twice can hit the cell. Particles scattered out of the beam can pass through a very thin–walled (0.3mm) stainless-steel exit window on their way to the detector. The "wakefield suppressors" provide smooth electrical continuity of the beam pipe around the beam, so that the target chamber does not act as an inadvertant resonant cavity and absorb energy from the beam.

Cryogenic Polarized ^{3}He Internal Gas Target

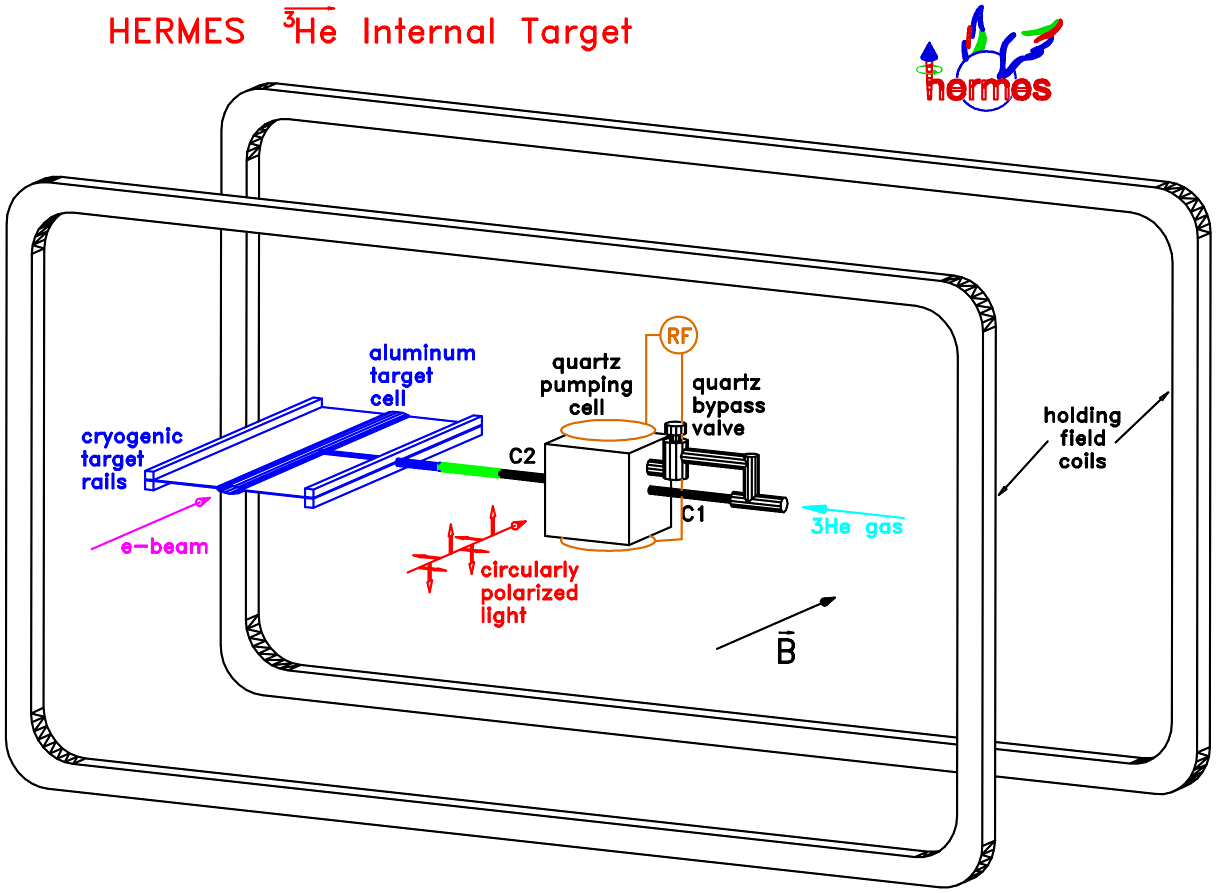

High–purity ^{3}He gas flows into a quartz pumping cell, where the atoms are excited to a metastable state *via* a radio–frequency signal. Circularly polarized light polarizes the nuclei of those atoms in the metastable state. When metastable atoms collide with ground-state atoms, they can exchange electron states. In this way, a population of ground state atoms with polarized nuclei develops, with a risetime of about 10-15 seconds. A fraction of the polarized atoms in the pumping cell will be excited by the RF and subsequently decay by photon emission; a polarimeter (not shown) observes these photons and thus measures the polarization of atoms in the pumping cell.

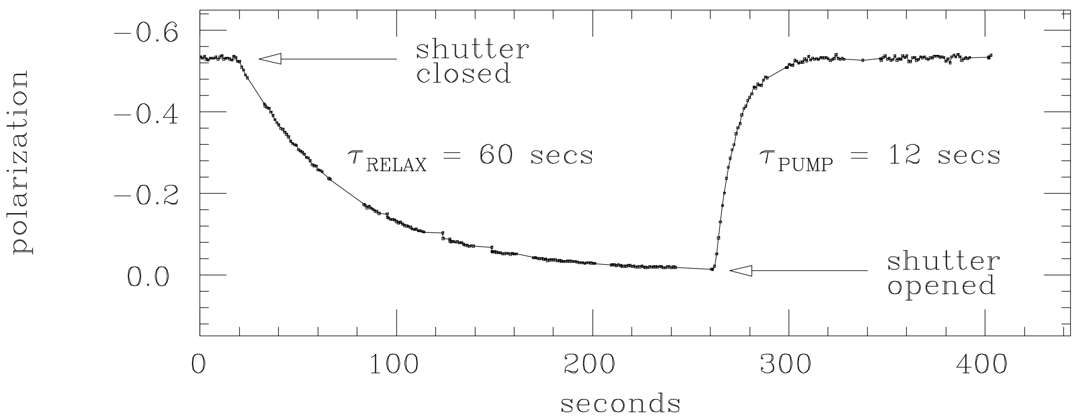

Internal Atomic Hydrogen Gas Target

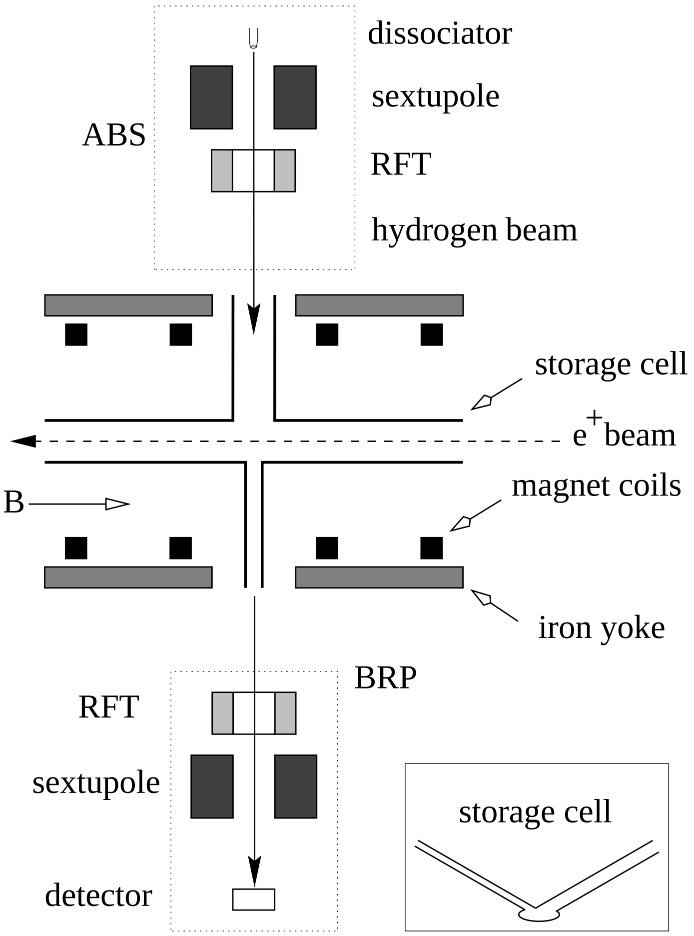

In the atomic beam source (ABS), molecular hydrogen gas is dissociated into atomic hydrogen which then passes through an electromagnetic system (RFT) producing atoms with a nearly equal population of the

$$|\text{proton} \uparrow \quad \text{electron} \uparrow>$$

and

$$|\text{proton} \uparrow \quad \text{electron} \downarrow>$$

states, so that the electrons are unpolarized. The polarization of the protons is nearly 100% before entering the storage cell. Some of the atoms travel out of the storage cell into a Breit-Rabi polarimeter (BRP) which counts the numbers of atoms in these states.

Target Optical Monitor (TOM)

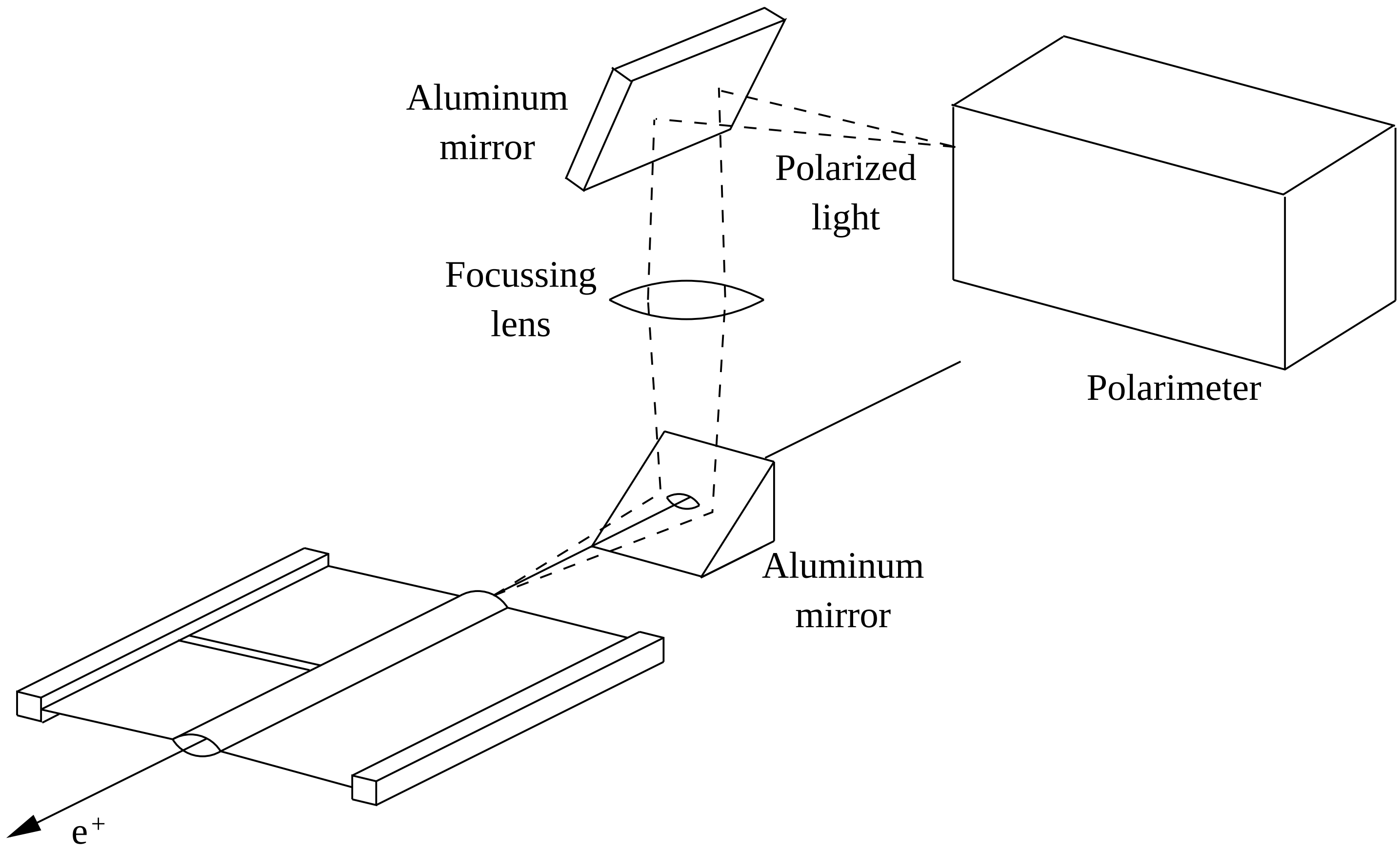

In addition to the dedicated polarimeters used by the ^{3}He and ^{1}H targets, another method is employed to observe the atoms in the storage cell – the Target Optical Monitor. The RF field induced by the passing beam packets can excite the atoms in the storage cell; if they decay by photon emission, those photons can be observed using the apparatus shown.

In the case of the ^{3}He target, this excitation and subsequent decay is exactly the same as that employed in the pumping cell, and so the polarimeter used in the TOM is of the same design. This provides a means to observe the polarization of the ^{3}He atoms both in the pumping cell and in the storage cell.

The HERMES Spectrometer

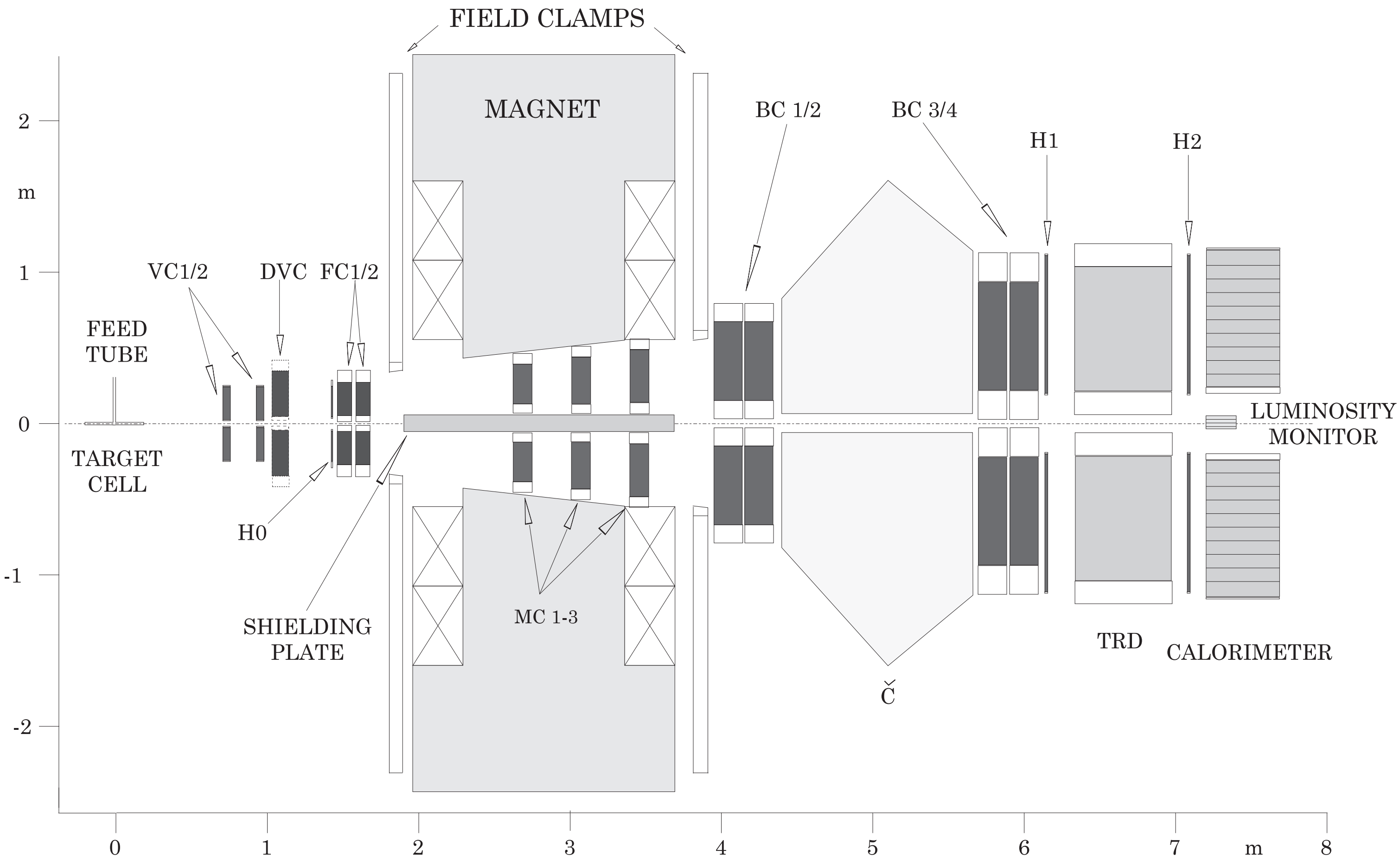

- Forward Tracking: Microstrip Vertex Chambers, Drift Vertex Chambers, Front Chambers, Magnet Chambers
- Back Tracking: Back Chambers
- Particle Identification: Cherenkov Detector, Transition Radiation Detector, Preshower (H2), Calorimeter; also Time-of-Flight (hodoscopes)
- Luminosity Monitor
- Fast Trigger: Scintillator Hodoscopes H0, H1, and H2; Calorimeter; Luminosity Monitor

Tracking Chambers

- Microstrip Vertex Chambers:

  high resolution measurement of the scattering angle and vertex position

  aluminum strips etched on a high-resistivity substrate form alternating cathode (85 μm) and anode (7 μm) lines; these face a cathode plane on the other gas of a 3 mm thick gas layer

  6 planes – VUXXVU – 65 μm resolution per plane

- Drift Vertex Chambers:

  increased acceptance for the muon physics program

  6 mm drift cell

  6 planes – XX'UU'VV' – 220 μm resolution per plane

- Front Drift Chambers:

  good spatial resolution immediately in front of the magnet

  7 mm drift cell

  12 planes – 2(UU'XX'VV') – 225 μm resolution per plane

- Magnet Chambers:

  standard proportional chamber

  0.5 mm wire separation

  9 planes – 3(UXV) – 700 μm resolution per plane

- Back Drift Chambers:

  tracking for momentum measurement

  15 mm drift cell

  24 planes – 4(UU'XX'VV') – 280 μm resolution per plane

Track Reconstruction

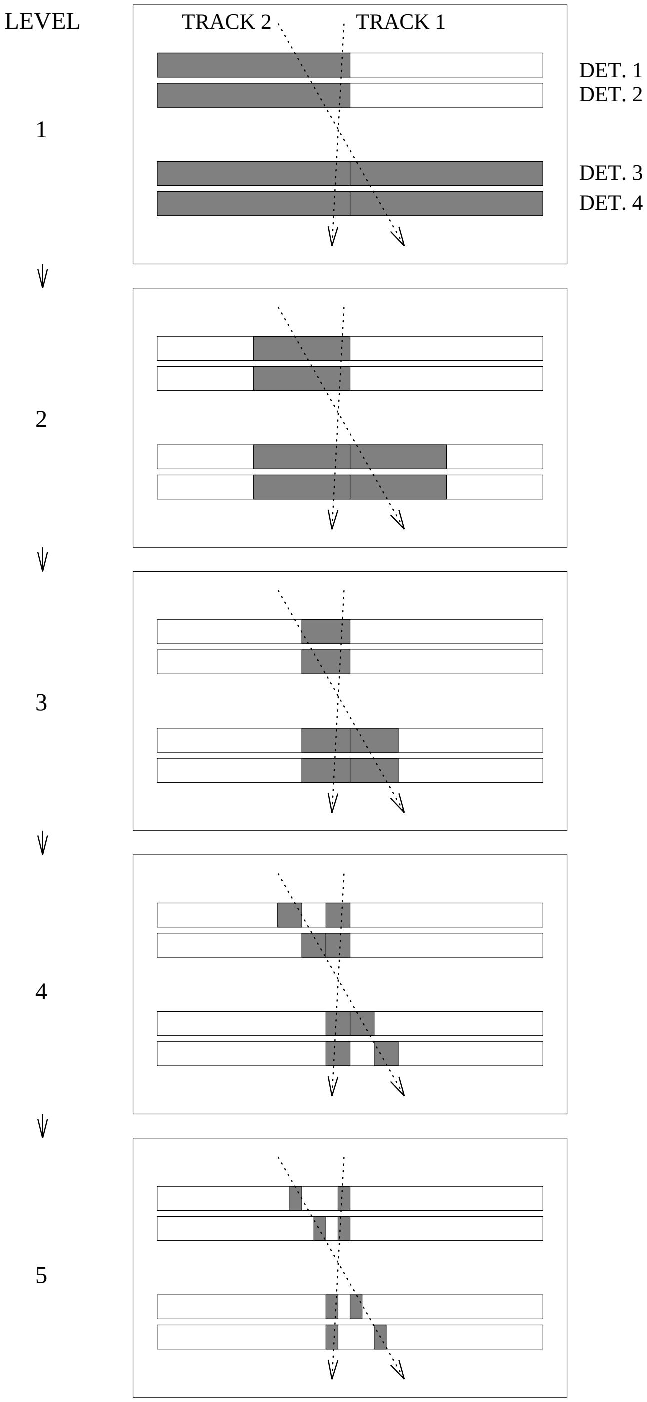

HERMES uses a fast "tree-search" algorithm to find tracks in the information provided by the tracking chambers. The resolution of each chamber plane is first made very poor and a search for tracks is done. Then, the resolution of each plane is improved by a factor of two, and a search for valid tracks **based on the results of the previous step** is done again. This process continues until the actual resolution of the chambers is reached. At each step, only valid hit patterns are allowed. If a "forbidden" hit pattern is revealed during a step, then the proposed track is abandoned.

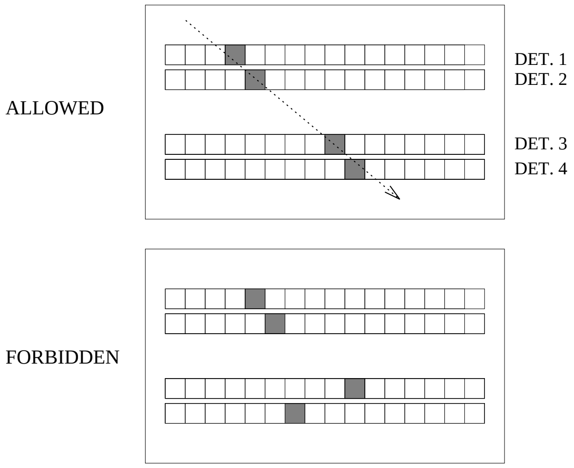

It is possible to store all valid hit patterns in a small database, by taking full advantage of this algorithm. At the full resolution, the total number of valid hit patterns is about 10^8! By basing each search step on the previous step, and by exploiting various symmetries, the number of stored hit patterns is reduced to about 50,000.

For the momentum reconstruction, the tracks in the front and back of the magnet have to be linked up to form a single track, then the momentum is calculated from the field integral and bend angle, using a fast look-up table.

Particle Identification Detectors

- Threshold Cherenkov Detector:

  1995: pure nitrogen gas was used, for which the $\pi/K/p$ momentum thresholds are 5.6/19.8/37.6 GeV respectively; therefore only detected pions and positrons in 1995, for detector commissioning purposes

  1996-1997: 70% N_2 + 30% C_4F_{10} gas was used, for which the $\pi/K/p$ momentum thresholds are 3.8/13.6/25.8 GeV respectively; better pion acceptance – a few kaons with 13.6 GeV momentum or more are there

  [present: Ring Imaging Cherenkov (RICH): much greater acceptance and identification for pions, kaons and protons]

- Transition Radiation Detector (TRD):

  transition radiation occurs when a charged particle of passes through an interface between two differing indices of refraction; only electrons and positrons will produce such radiation at HERMES energies

  6 planes – each plane is composed of a radiator followed by a 90% Xe + 10% CH_4 gas filled proportional counter which acts to detect the transition radiation X-rays

- Hodoscopes (H0, H1, H2):

  fast scintillator detectors, primarily for triggering

  11 mm thick Pb sheet ("preshower") in front of H2 enlarges the pulse height in H2 for electrons and positrons;

  can identify protons and deuterons below 2 GeV momentum via TOF

- Lead-Glass Calorimeter (CALO):

  designed to largely respond only to electrons and positrons, to aid in triggering and particle identification

  420 blocks of F101 lead-glass in 42x10 stacks, above and below the beam

  each block is 9x9x50 cm^3; 18 radiation lengths deep; $n = 1.65$

Particle Identification Performance

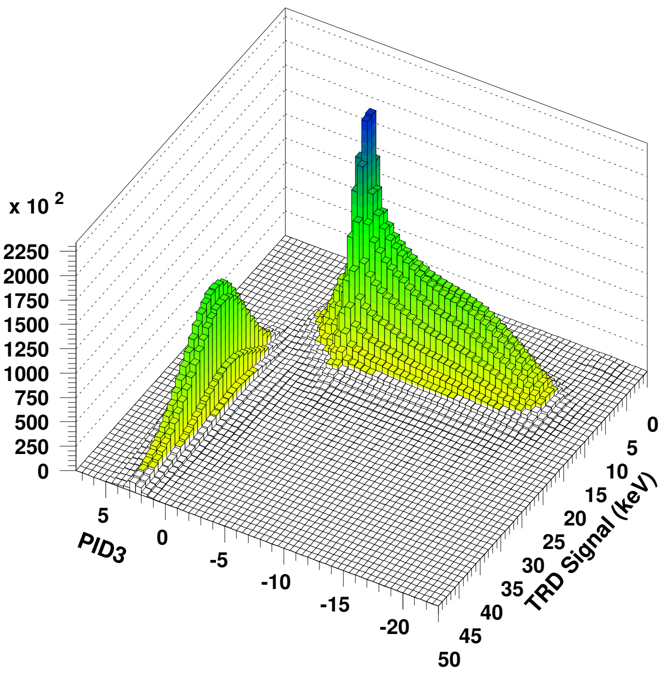

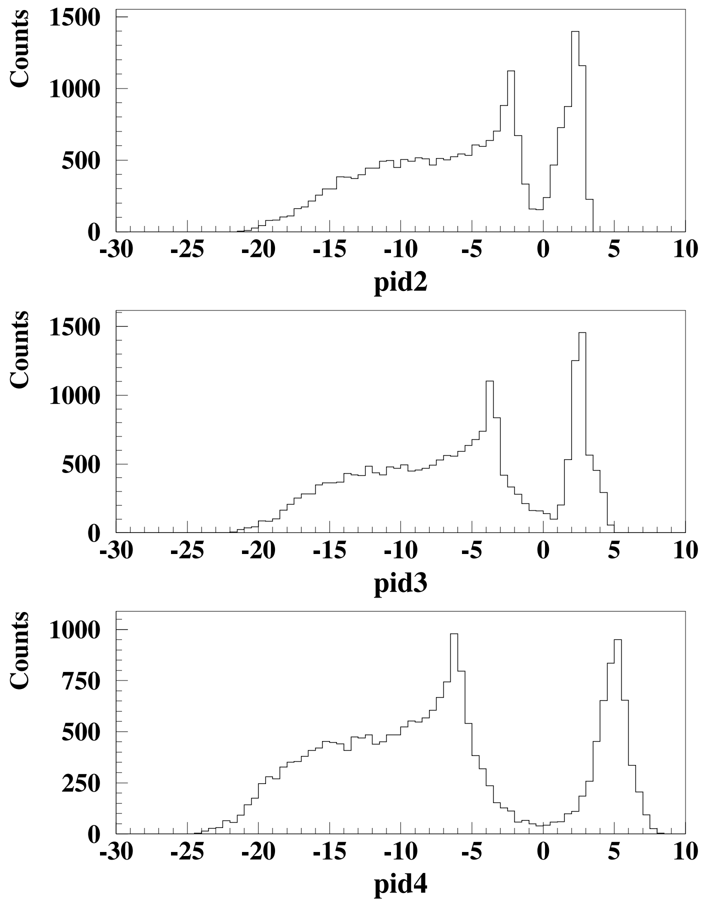

No single detector in the menu of HERMES can perform the full particle identification job alone – some scheme to let the detectors "vote" is needed. By comparing the responses of the various detectors, and by carrying out various calibrations, one can learn to calculate two numbers for each event and for each detector: the probability that a track corresponds to an electron or positron, P^{e}, and the probability that it is a hadron, P^{h}. These values can be combined into a single number, for example

$$\mathrm{PID3} = \log_{10}[(P^{\mathrm{e}}_{\mathrm{Cal}} P^{\mathrm{e}}_{\mathrm{Pre}} P^{\mathrm{e}}_{\mathrm{Che}})/\ (P^{\mathrm{h}}_{\mathrm{Cal}} P^{\mathrm{h}}_{\mathrm{Pre}} P^{\mathrm{h}}_{\mathrm{Che}})]$$

which can be used to make a single cut to distinguish electrons and positrons from hadrons. (PID3<0 implies a hadron.) The PID2 number only uses only the calorimeter and preshower, while PID4 uses the calorimeter, preshower, Cherenkov, and TRD signals. In 1995, for about 97% of our events, we are able to make a cut on the 2D plot of TRD *vs.* PID3 above. This provides an electron or positron identification with 1% or less hadron contamination.

Luminosity Monitor (LUMI)

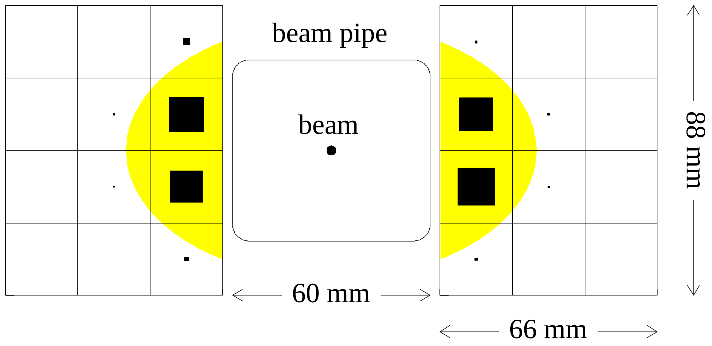

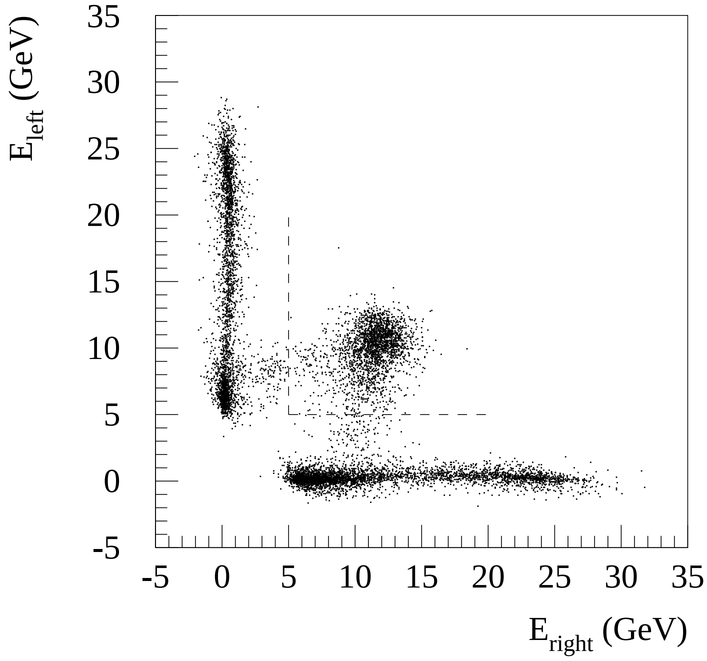

HERMES uses many target gases, and we need to have a monitor of the beam-target luminosity which is somewhat independent of the target in use. Since all target gases contain electrons (!), we can observe elastic scattering of the beam particles from these electrons and use that as our luminosity monitor. Elastic scattering of positrons and electrons (Bhabha scattering), or of electrons and electrons (Moller scattering), is observed by placing two small $NaBi(WO_4)_2$ calorimeters on either side of the beam and requiring a coincidence between two signals of approximately equal energy, about half the beam energy each – this corresponds to elastic scattering at about $\theta_{CM} = 90°$.

In order that the luminosity yield not have a spin-dependent component (fatal to any spin-asymmetry measurement), it is important that the electrons in the target not be polarized. For the ^{3}He target, this is not an issue. For the ^{1}H target, the RF system must produce equal populations of atoms with parallel and anti-parallel electron spins, but during normal operations this is not hard to achieve. Conversely, it is possible to produce electron polarization in the target on purpose and then use the resulting asymmetry in the luminosity yield to check on the operation of the ^{1}H target.

Physics Triggers

- Deep Inelastic Trigger: This is the primary trigger for HERMES, and all the results shown in this set of talks are based on it. We look for a scattered beam particle (positron beam during 1995-1997, electron beam in 1998-1999) with an energy of at least 3.5 GeV. (The beam energy is 27.5 GeV). The detector requirement is then: All four of H0, H1, H2, and CALO must fire in the correct time relationship, with the additional requirement that the CALO must record at least 3.5 GeV of energy (at least in 1995 – this was later reduced to 1.4 GeV). Only an electron or positron can produce any significant light output in the calorimeter.

- Photoproduction Trigger: We also seek to study some physics processes in which the scattered beam particle is not observed. This usually means that the beam particle was deflected at such a small angle that it “went down the beam pipe” and missed the spectrometer altogether. At such small angles, the virtual photon produced is almost a real photon, hence the name for this type of trigger. Lacking the scattered beam particle, we look for one or more secondary particles (pions and the like) using some combination of hodoscopes and prompt wire chamber information.

- Luminosity Trigger: A simple coincidence between the left and right luminosity detector clusters.

- Other triggers: A variety of triggers under test and development are always in use. For example, triggering on a coincidence between one lumi cluster and a “hadron” in the main detector increases our acceptance for low-Q^2 events.

Monte Carlo

For both the design of a detector and the analysis of the data from it, a Monte Carlo simulation of the detector operation is needed. No true understanding of the detector can be claimed until the response of the detector in reality and in the simulation reasonably agree.

Such simulations are usually broken down into three stages.

1. Event Generation: To properly simulate the interactions occuring between beam and target particles, programs must be written which produce random sequences of kinematically final states. These programs must contain the proper cross sections so that the relative numbers of each kind of event that occur are correct. The events must also be properly distributed in phase space.

2. Particle Propagation through the Detector: The particles produced by the event generator are allowed to travel through the detector. This usually means that the particles will lose energy and/or generate additional secondary particles which also have to be tracked. The production of light (e.g. in scintillators) and ions (e.g. in wire chamber gases) must be tracked so that the total response of each detector can be calculated.

3. Digitization: Now that the total amount of light/charge/whatever deposited in each detector has been calculated from the passage of primary and secondary particles through the detector volume, those values must be converted into numbers such as are produced in the digitizing electronics of the real detector. Those numbers are then packaged into an "event" suitable for storage on disk or tape. The analysis package used for real data can then be used for this simulated data as well.

Agreement of Monte Carlo and Data

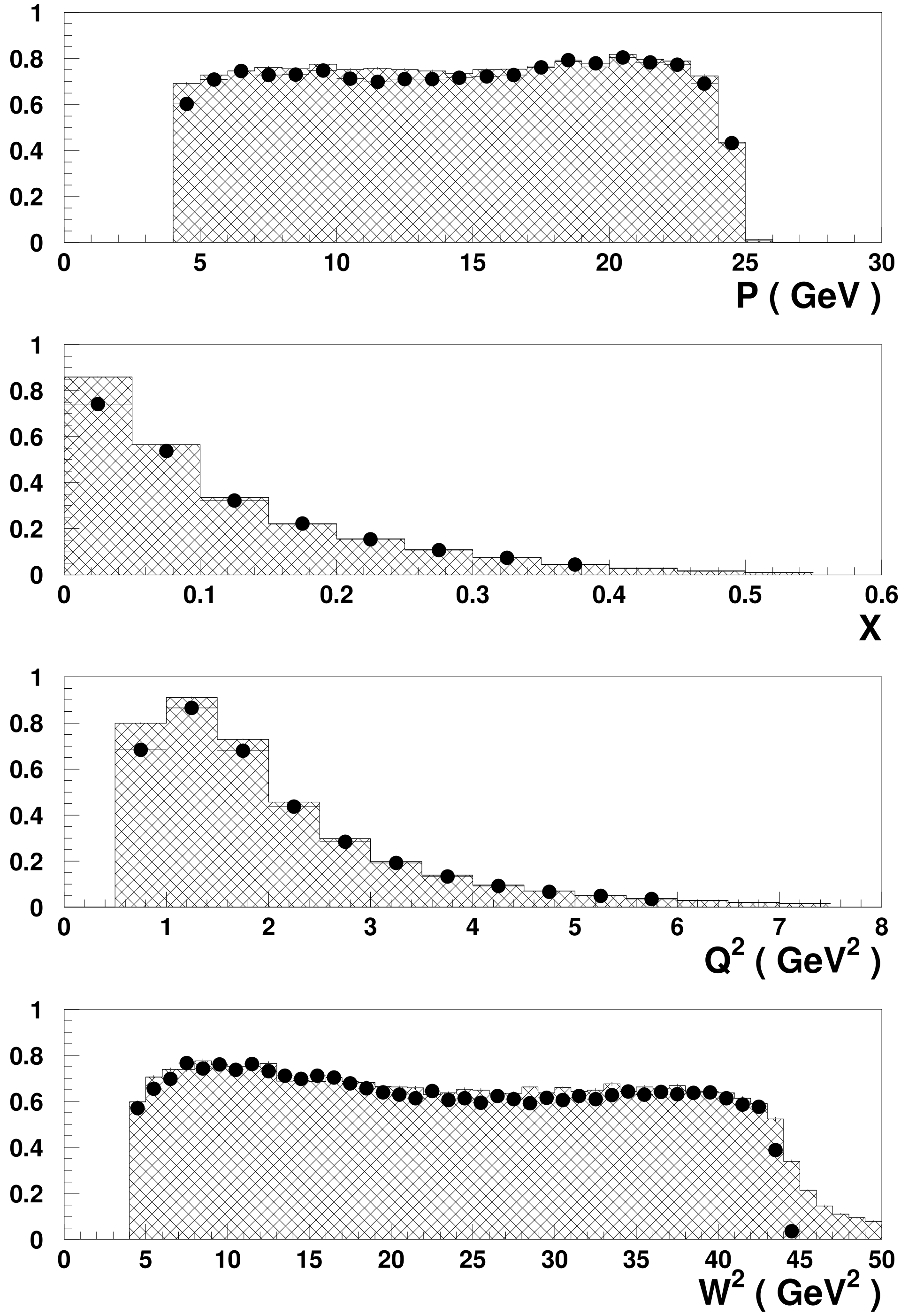

Shaded area is Monte Carlo – points are data. The agreement is quite good except at the very edges of the acceptance. (Vertical scale is arbitrary.)

Resolutions Derived from Monte Carlo

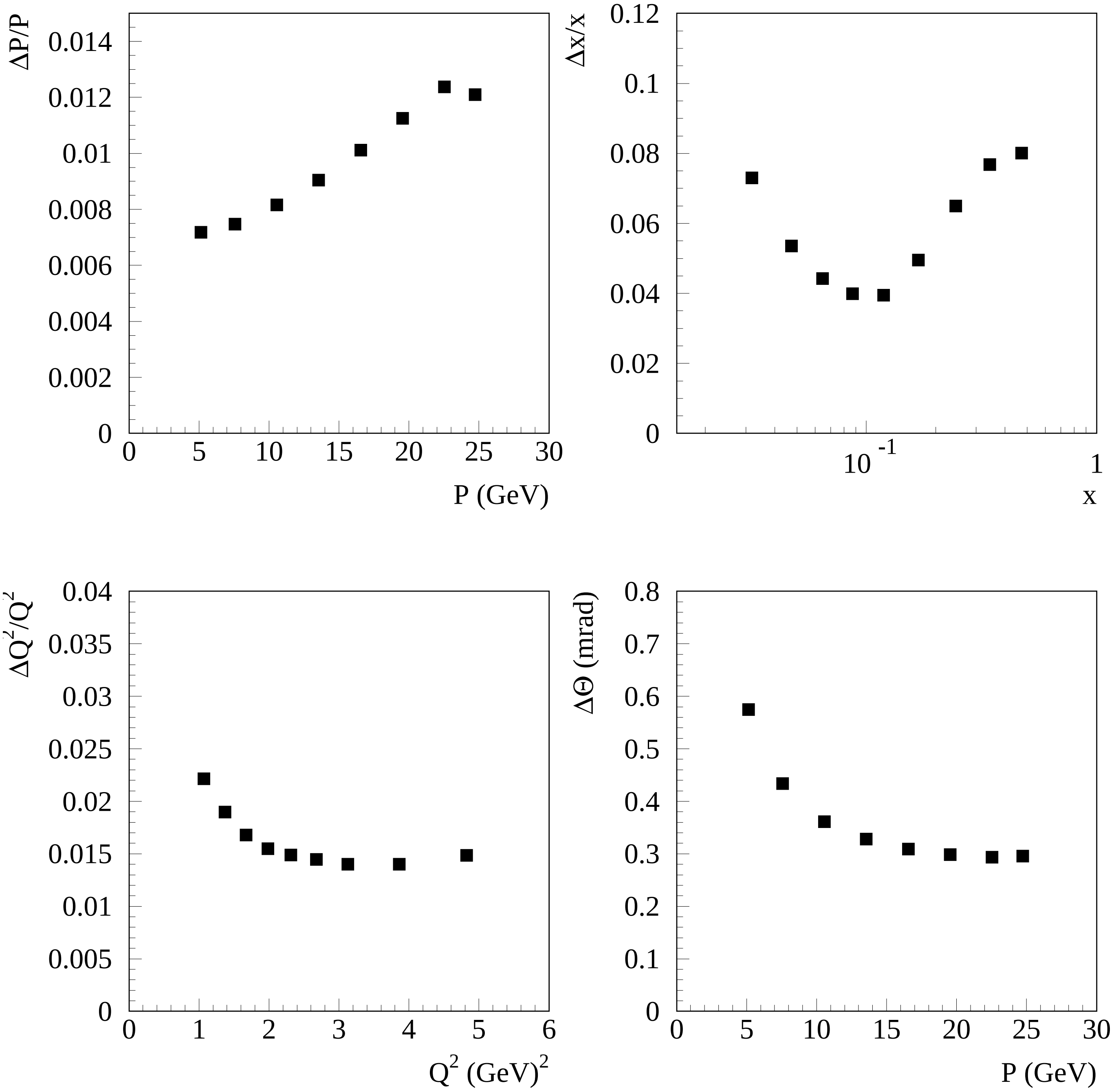

Event Display

(DIS event with K_s in hadronic final state):

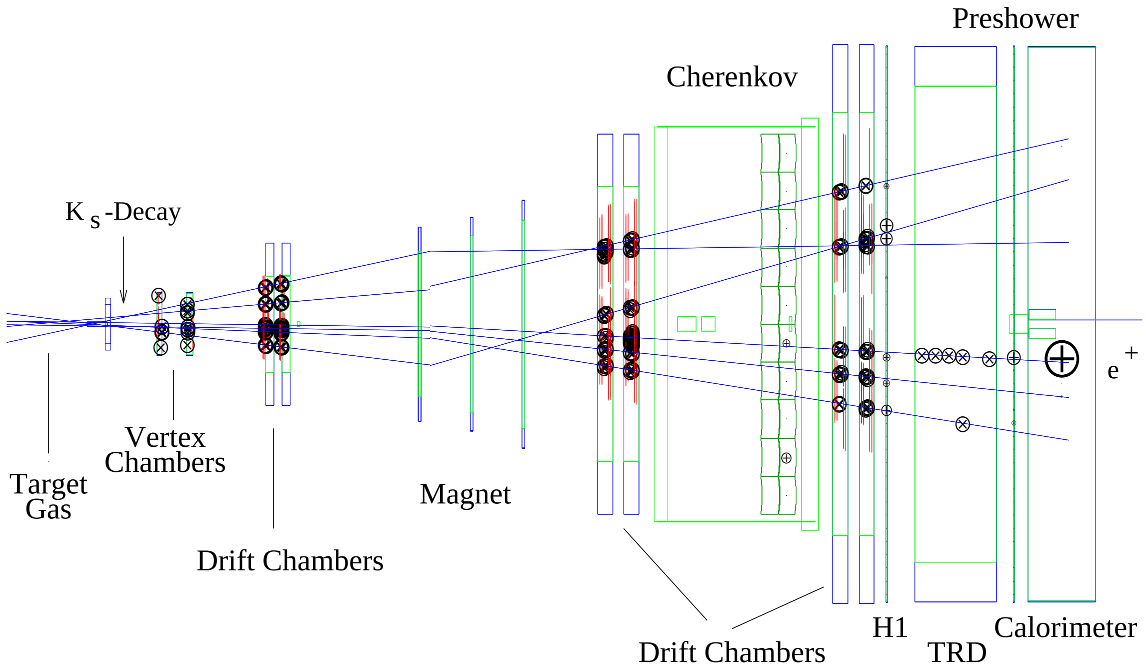

transverse vertex distribution: K_s mass peak:

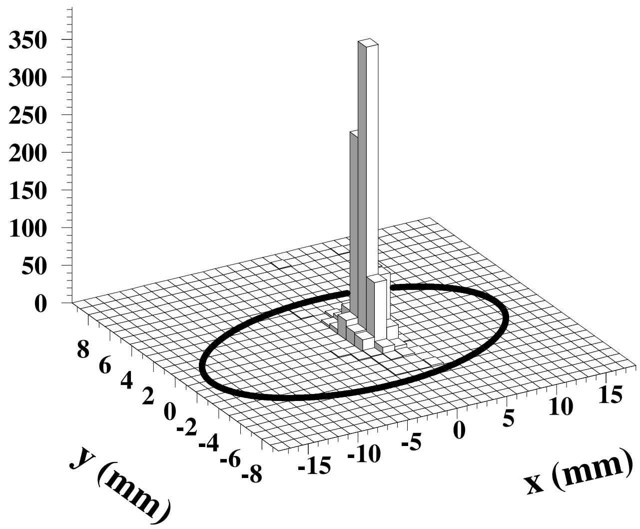

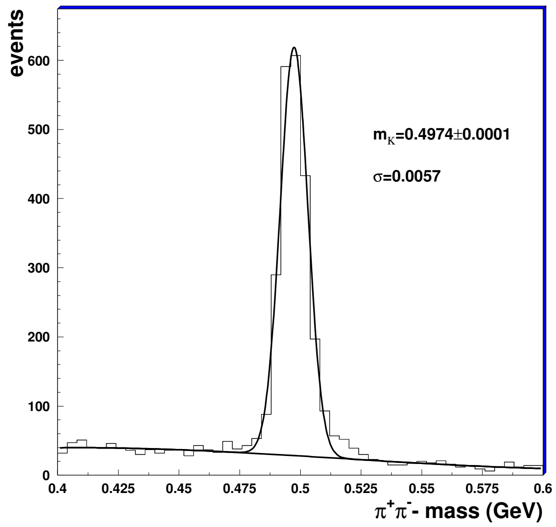

no background from wall scattering!

Exemplary HERMES event, in which a K-short is produced by a deep inelastic process, decays to two pions, and is reconstructed from the two pion tracks. The distribution of vertices in the target–beam interaction region (summed over many events) shows no evidence of scattering from the target cell walls.

HERMES Acceptance

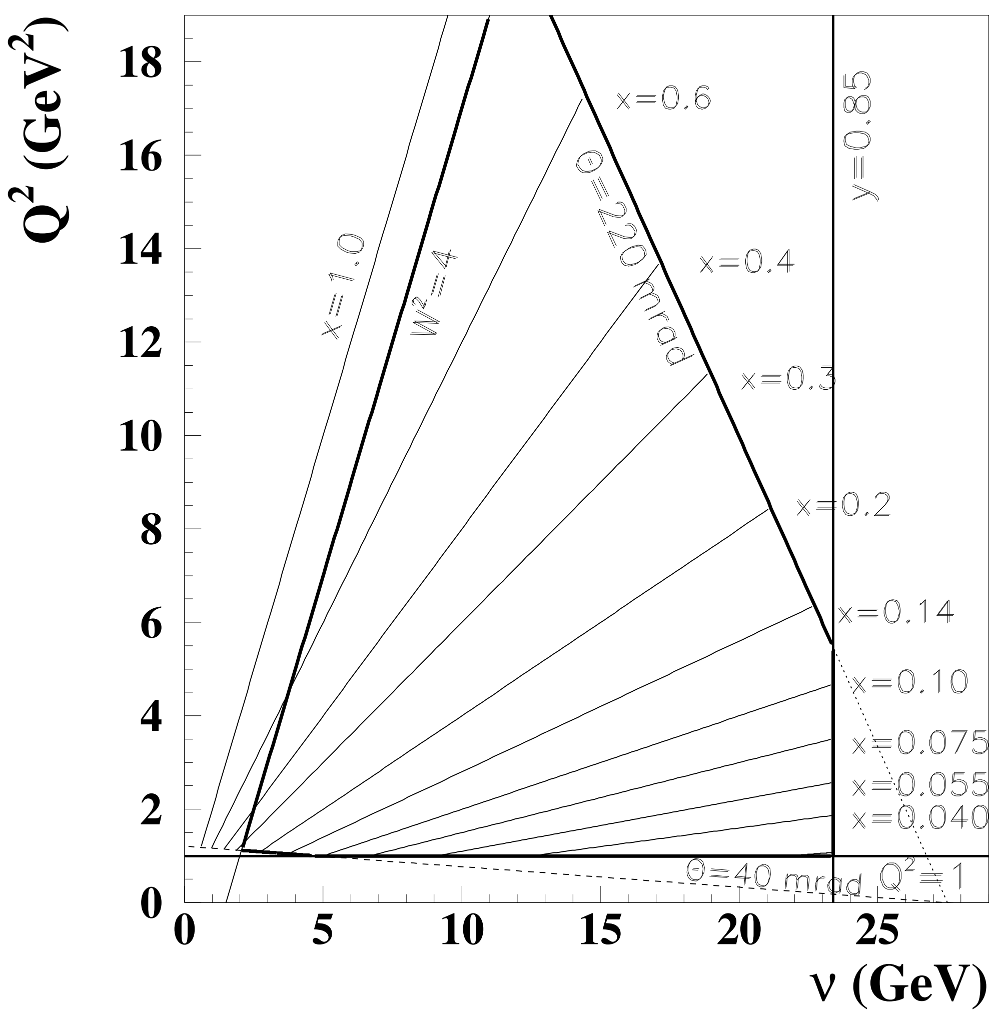

The HERMES acceptance for deep inelastic events is defined by four kinematic cuts:

- Scattering angle: 40 mrad $< \Theta <$ 220 mrad
  these are the physical limits of the useful detector acceptance
- Virtual Photon Energy Fraction: $y = \nu/E < 0.85$
  this avoids a region of very large radiative corrections
- Photon-Nucleon Invariant Mass: $W^2 > 4$ GeV^2
  this avoids a region of strong hadronic resonances
- Momentum Transfer Squared: $Q^2 > 1$ GeV^2
  this provides enough momentum transfer to justify the impulse approximation

where the events actually go...

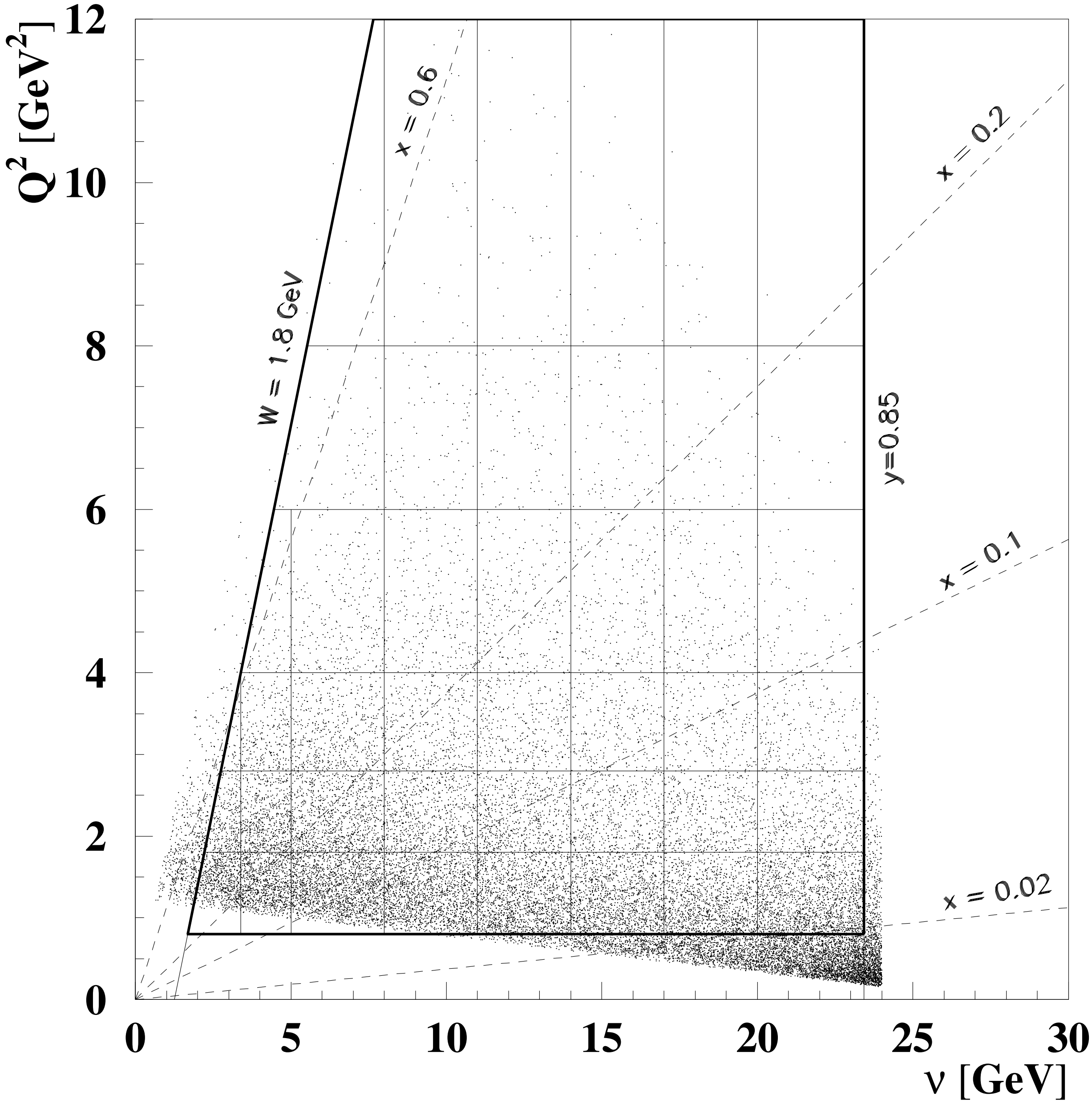

The Gottfried Sum Rule

The Gottfried Sum Rule is an integral over the difference in the F_2 structure functions of the proton and neutron:

$$\begin{aligned} S_\mathrm{G} &= \int_0^1 \frac{dx}{x}\left(F_2^p(x) - F_2^n(x)\right) \\ &= \int_0^1 dx \left(\sum_f e_f^2 q_f^p(x) - \sum_f e_f^2 q_f^n(x)\right) \\ &= \int_0^1 dx \left(\frac{4}{9}u^p(x) + \frac{1}{9}d^p(x) + \frac{1}{9}s^p(x) + \frac{4}{9}\bar{u}^p(x) + \frac{1}{9}\bar{d}^p(x) + \frac{1}{9}\bar{s}^p(x)\right) \\ &\qquad - \left(\frac{4}{9}u^n(x) + \frac{1}{9}d^n(x) + \frac{1}{9}s^n(x) + \frac{4}{9}\bar{u}^n(x) + \frac{1}{9}\bar{d}^n(x) + \frac{1}{9}\bar{s}^n(x)\right) \end{aligned}$$

We will assume isospin symmetry is valid – switching the n and p labels just means switching u and d quarks:

$$\begin{array}{lll} u^p(x) = d^n(x) \equiv u(x) & d^p(x) = u^n(x) \equiv d(x) & s^p(x) = s^n(x) \\ \bar{u}^p(x) = \bar{d}^n(x) \equiv \bar{u}(x) & \bar{d}^p(x) = \bar{u}^n(x) \equiv \bar{d}(x) & \bar{s}^p(x) = \bar{s}^n(x) \end{array}$$

Now we define the valence quark distributions:

$$u_v(x) \equiv u(x) - \bar{u}(x) \qquad d_v(x) \equiv d(x) - \bar{d}(x)$$

Then the Gottfried sum takes this form:

$$\begin{aligned} S_\mathrm{G} &= \frac{1}{9}\int_0^1 dx (4u(x) + d(x) + 4\bar{u}(x) + \bar{d}(x) \\ &\qquad - 4d(x) - u(x) - 4\bar{d}(x) - \bar{u}(x)) \\ &= \frac{1}{3}\int_0^1 dx\,(u(x) - d(x)) + \frac{1}{3}\int_0^1 dx\,(\bar{u}(x) - \bar{d}(x)) \\ S_\mathrm{G} &= \frac{1}{3}\int_0^1 dx\,(u_v(x) - d_v(x)) + \frac{2}{3}\int_0^1 dx\,(\bar{u}(x) - \bar{d}(x)) \end{aligned}$$

If we now further assume that the light quark sea is flavor symmetric

$$\bar{u}(x) = \bar{d}(x)$$

then the Gottfried sum is reduced to

$$S_\mathrm{G} = \frac{1}{3}\int_0^1 dx\,(u_v(x) - d_v(x)) = \frac{1}{3}(2-1) = \frac{1}{3}$$

The Gottfried Sum Rule (more)

In the early 1990's, the New Muon Collaboration (NMC) measured $F_2^p(x)$ and $F_2^d(x)$ in inclusive deep inelastic scattering of unpolarized muons from hydrogen and deuterium targets. From $F_2^p(x)$ and $F_2^d(x)$ they are able to extract $F_2^n(x)$ (by assuming that $F_2^d(x) = (F_2^p(x) + F_2^n(x))/2$), and hence the Gottfried sum. In 1994 they published a value of

$$S_{\mathrm{G}} = 0.235 \pm 0.026.$$

Assuming that isospin symmetry is still valid, then this measurement suggests that the light quark sea is not flavor symmetric after all, i.e. $\bar{u}(x) \neq \bar{d}(x)$.

Two methods are available to study the x-dependence of these unpolarized anti-quark distributions:

- the Drell-Yan process, as employed in CERN Experiment NA51 and Fermilab Experiment E866
- semi-inclusive deep inelastic scattering, as in HERMES

In semi-inclusive deep inelastic scattering, we must consider the fragmentation functions.

The Drell-Yan Process: $pN \to \mu^+\mu^- X$

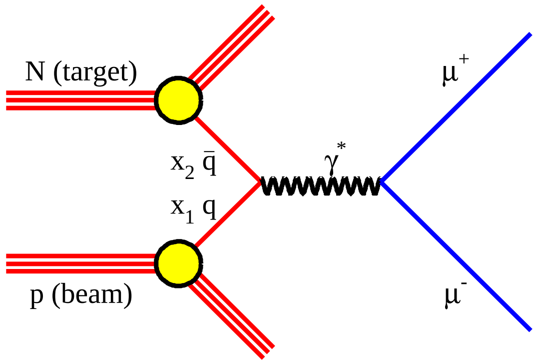

- Directly sensitive to antiquark distributions.

$$\sigma^{pN} \propto \sum_i e_i^2 \left[q_i(x_1)\bar{q}_i(x_2) + \bar{q}_i(x_1)q_i(x_2)\right]$$

$$2p_L/\sqrt{s} = x_1 - x_2 \equiv x_F \text{ and } M^2_{\mu^+\mu^-} = s x_1 x_2$$

- Compare Drell-Yan yields from nuclear targets (Liquid H_2 and D_2) and extract $\bar{u}/\bar{d}$. if charge symmetry is assumed.

$$\left.\frac{\sigma^{pd}}{2\sigma^{pp}}\right|_{x_F>>0} \approx \frac{1}{2}\left[1 + \frac{\bar{d}(x)}{\bar{u}(x)}\right]$$

- NA51 $\Rightarrow$ 6,000 events at $x = 0.18$ and $x_F \simeq 0$
PLB **332** 224 (1994)

$$\frac{\bar{u}}{\bar{d}} = 0.51 \pm 0.04 \pm 0.05$$

Why Drell-Yan and Semi-Inclusive Deep Inelastic Scattering can explore the same physics

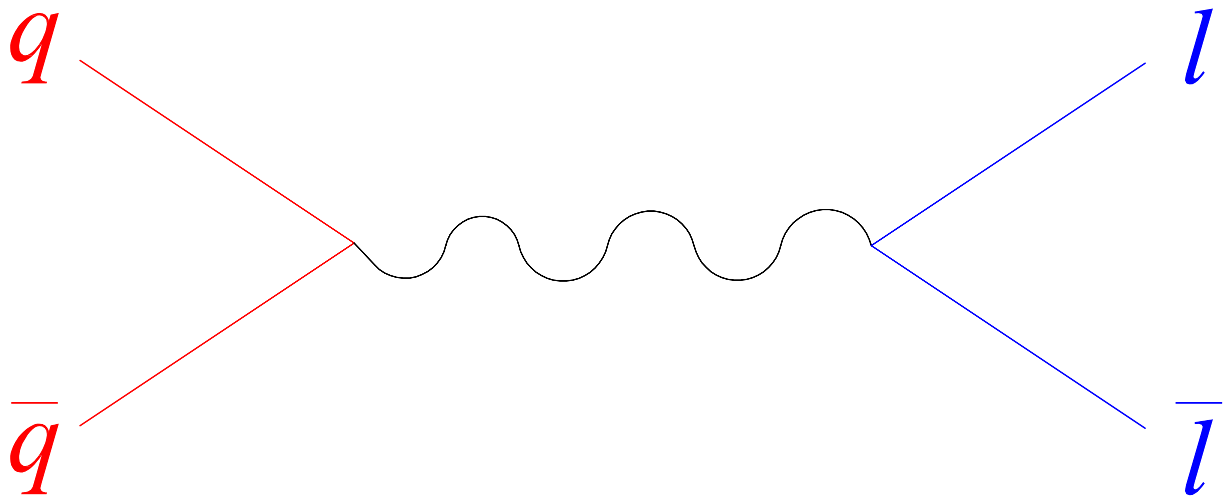

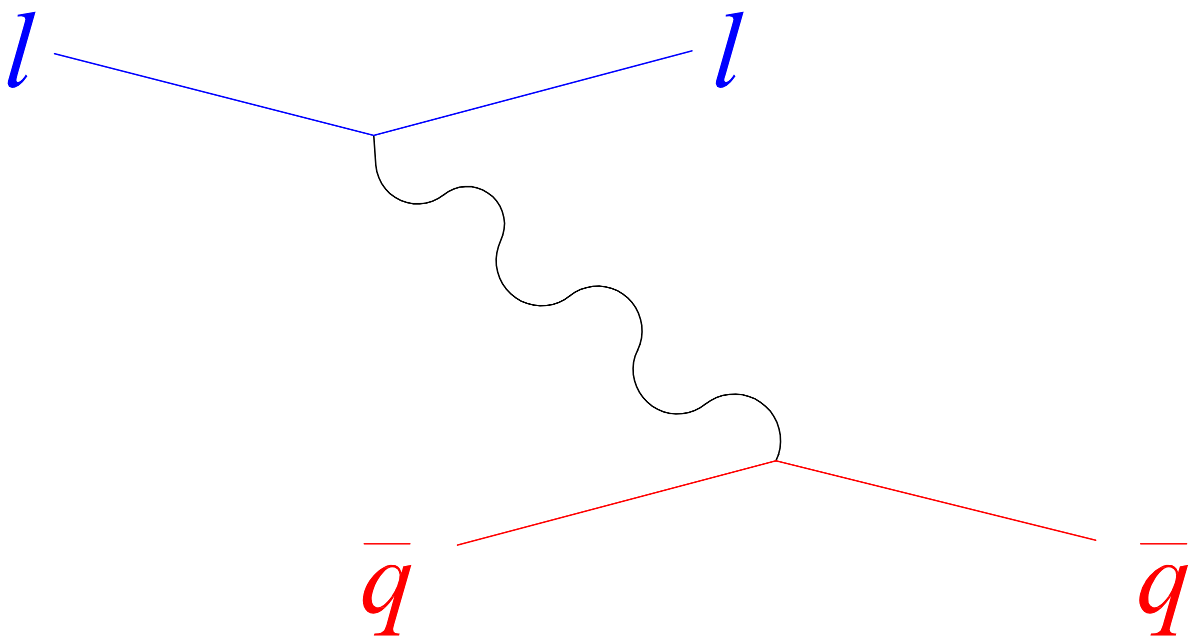

Fragmentation Functions

Recall that the number of hadrons of type h (pion, kaon, lambda...) produced is

$$N^h(x,z) \propto \sum_f e_f^2 q_f(x) D_f^h(z),$$

where $D_f^h(z)$ is the fragmentation function, expressing the probability that a quark of flavor f will produce a hadron of type h with energy fraction $z = E^h/\nu$, the fraction of the virtual photon energy carried away by the hadron.

Given that there are six types of quarks commonly found in the nucleon (u, $\bar{u}$, d, $\bar{d}$, s, $\bar{s}$) and two kinds of charged pions (π^+, π^-), then in principle there are 12 fragmentation functions for the production of charged pions from the nucleon. Application of charge and isospin symmetries leaves only three independent fragmentation functions:

$$\begin{aligned}
D^+(z) &= D_u^{\pi^+}(z) = D_d^{\pi^-}(z) = D_{\bar{d}}^{\pi^+}(z) = D_{\bar{u}}^{\pi^-}(z) && \text{“favoured''} \\
D^-(z) &= D_d^{\pi^+}(z) = D_u^{\pi^-}(z) = D_{\bar{u}}^{\pi^+}(z) = D_{\bar{d}}^{\pi^-}(z) && \text{“unfavoured''} \\
D_s(z) &= D_s^{\pi^+}(z) = D_s^{\pi^-}(z) = D_{\bar{s}}^{\pi^+}(z) = D_{\bar{s}}^{\pi^-}(z) && \text{“strange''}
\end{aligned}$$

These functions are hard enough to measure – you have to build a big accelerator like CERN or HERA and then a detector apparatus like HERMES. But calculating them is nearly impossible. Deep inelastic scattering is (by definition) done at a high enough energy to be treated perturbatively, but the subsequent fragmentation of the quarks into hadrons is strictly non-perturbative, and therefore a struggle to calculate.

As a result, if your experimental program depends on a knowledge of the fragmentation functions, you are going to have to measure them first – no theory can give them to you.

The Light Quark Sea Flavor Asymmetry from Semi-Inclusive Deep Inelastic Scattering

The flavor asymmetry is extracted from the observed ratio in the difference between pion yields from the proton and neutron data,

$$r(x,z) = \frac{N_p^{\pi^-} - N_n^{\pi^-}}{N_p^{\pi^+} - N_n^{\pi^+}}$$

where the normalized yield of pions from a proton or neutron target is

$$N^{\pi^\pm}(x,z) \propto \sum_f e_f^2 q_f(x) D_f^{\pi^\pm}(z)$$

as before. Using isospin symmetry and the definitions of the fragmentation functions listed previously, you can show that

$$\frac{1+r(x,z)}{1-r(x,z)} = \frac{u(x) - d(x) + \bar{u}(x) - \bar{d}(x)}{u_v(x) - d_v(x)} J(z)$$

where

$$J(z) = \frac{3}{5}\left(\frac{1 + D^-/D^+(z)}{1 - D^-/D^+(z)}\right).$$

The equation giving $r(x,z)$ is a product of two factors, one only a function of x, the other only a function of z. Those two factors can be extracted separately by fitting the data for $r(x,z)$ along x and z independently, **if factorization is valid.**

In this way the fragmentation function ratio $D^-/D^+(z)$ and the light quark sea asymmetry are determined together. The result for the fragmentation function ratio $D^-/D^+(z)$ is consistent with a previous EMC measurement.

HERMES Results for the Charged Pion Fragmentation Functions

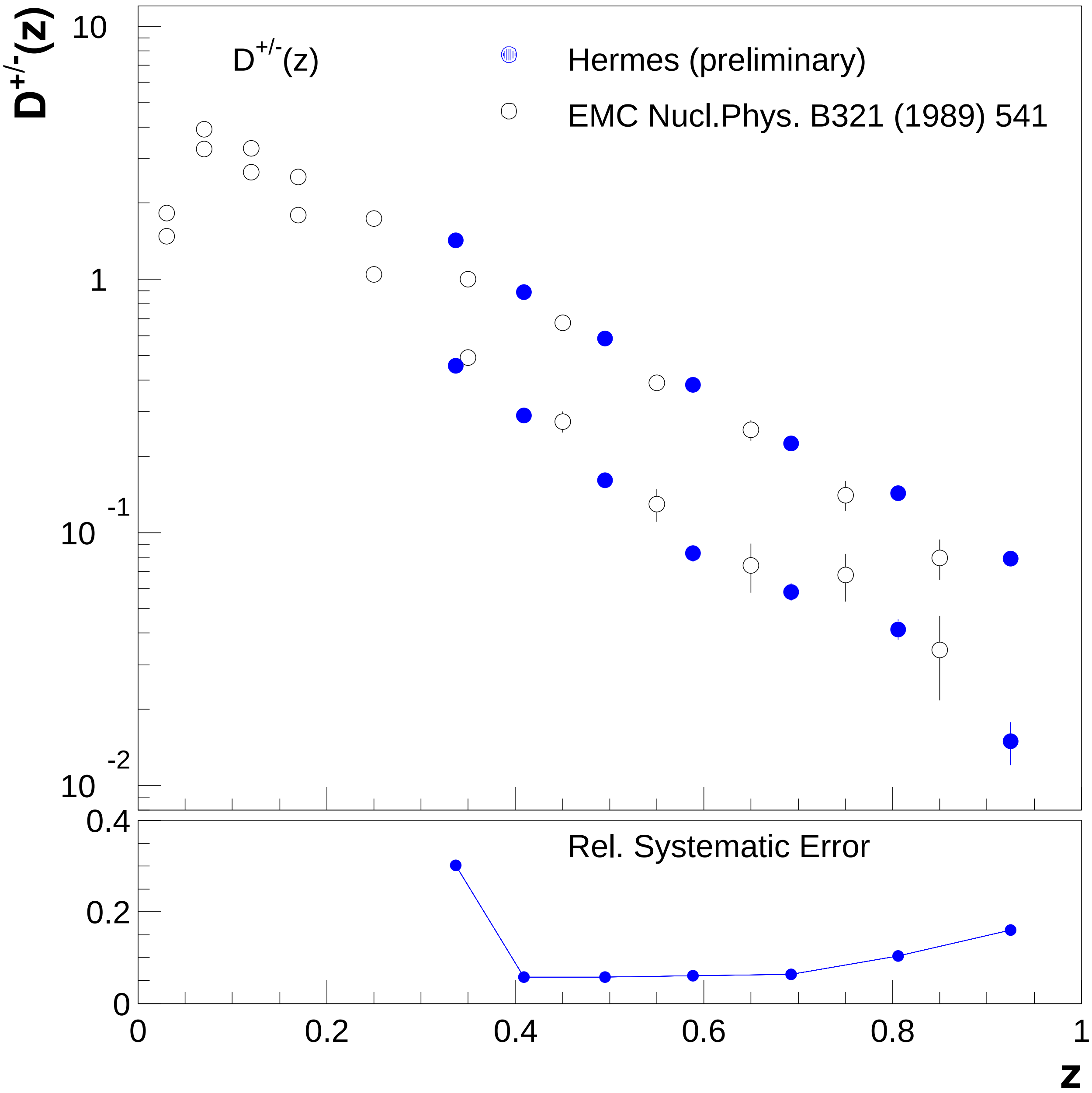

Favoured and unfavoured fragmentation functions *vs.* z measured at HERMES, in comparison to results from the EMC experiment.

Check on Factorization

The quantity of interest for the light quark sea asymmetry is

$$\frac{\bar{d}(x) - \bar{u}(x)}{u(x) - d(x)} = \frac{J(z)[1 - r(x,z)] - [1 + r(x,z)]}{J(z)[1 - r(x,z)] + [1 + r(x,z)]}.$$

As a check on **factorization**, we extract this quantity as a function of z for different values of x. Clearly, there is no dependence on z for any value of x.

$\Rightarrow$ Factorization is valid!

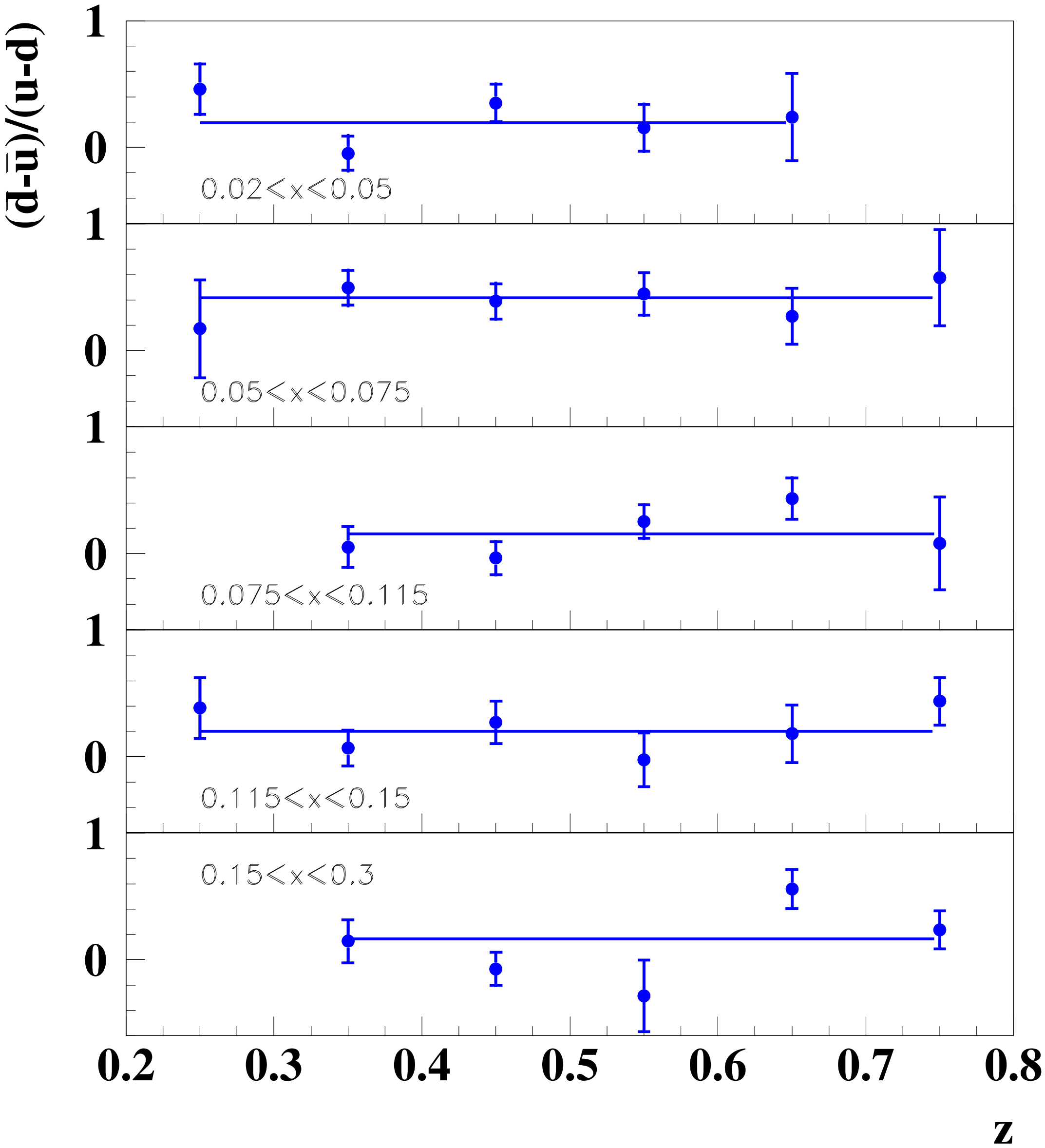

HERMES Results for the Light Quark Sea Flavor Asymmetry

The final HERMES results for

$$\frac{\bar{d}(x) - \bar{u}(x)}{u(x) - d(x)} = \frac{J(z)[1 - r(x,z)] - [1 + r(x,z)]}{J(z)[1 - r(x,z)] + [1 + r(x,z)]}$$

are published in K. Ackerstaff *et al.* (The HERMES Collaboration), Phys. Rev. Lett. 81 (1998) 5519. The results confirm the asymmetric nature of the light quark sea.

HERMES measures $\frac{\bar{d}(x)-\bar{u}(x)}{u(x)-d(x)}$ directly, while the Drell-Yan experiment E866 at Fermilab measures $\bar{d}/\bar{u}$. To calculate the Gottfried sum, $\bar{d}(x) - \bar{u}(x)$ is needed, and so some transformations of both data sets are required.

- HERMES calculates $\bar{d}(x) - \bar{u}(x)$ from $\frac{\bar{d}(x)-\bar{u}(x)}{u(x)-d(x)}$ by using parametrizations of the $u(x)$ and $d(x)$ distributions of M. Glück *et al.* [Z. Phys. **C67** 433 (1995)], “GRV 94 LO”.
- E866 calculates $\bar{d}(x) - \bar{u}(x)$ from $\bar{d}/\bar{u}$ by using the “CTEQ4M” [H.L. Lai *et al.*, Phys. Rev. **D55** 1280 (1997)] parametrization of $\bar{d}(x) + \bar{u}(x)$.

Using $\bar{d}(x)-\bar{u}(x)$ as a common quantity for comparison, we see that the HERMES and E866 data are in agreement. This is significant because:

- The two experiments use **very** different experimental techniques.
- The momentum transfer, Q^2, of each experiment is very different as well.

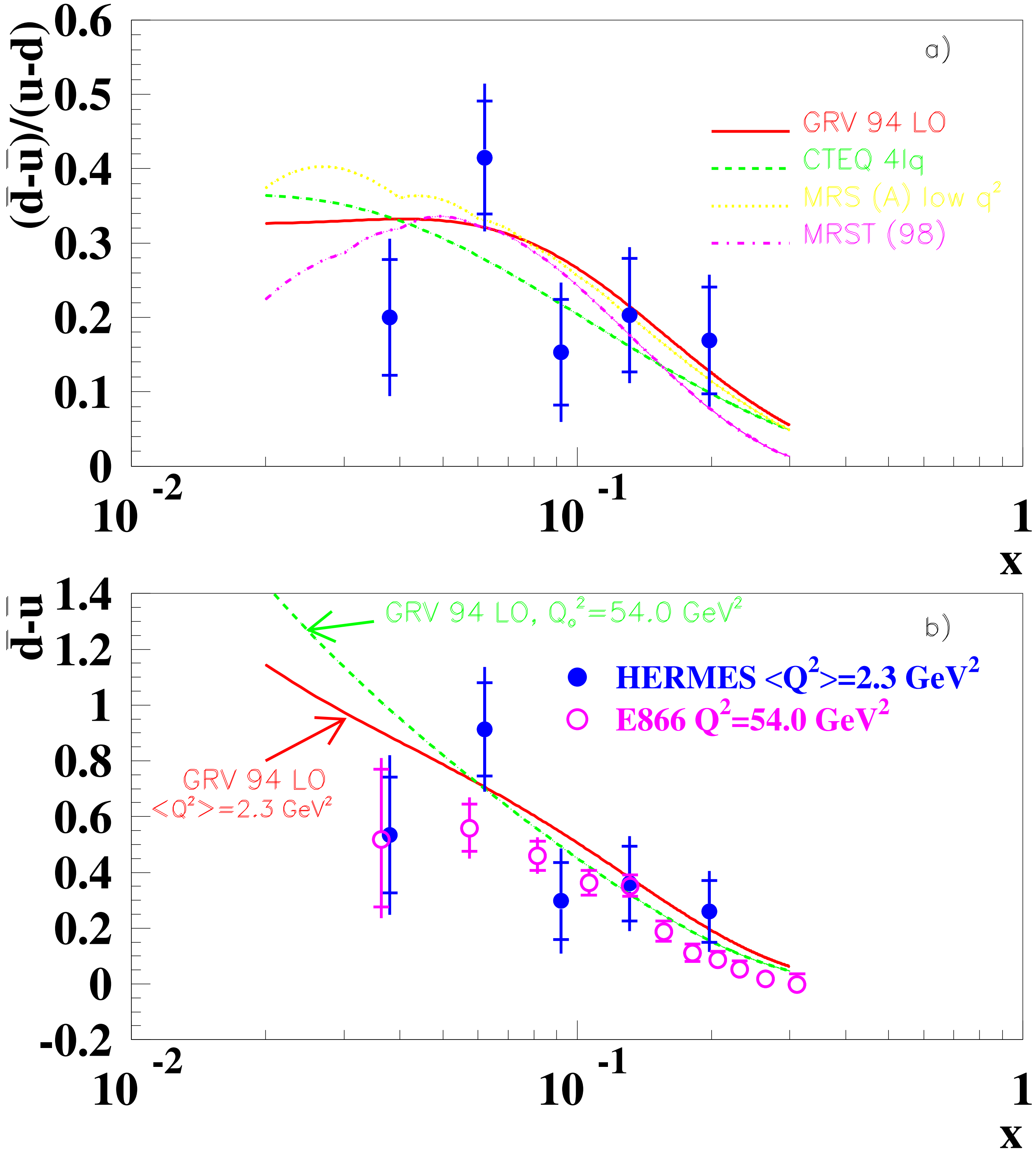

a)
$(\bar{d}-\bar{u})/(u-d)$
GRV 94 LO
CTEQ 4lq
MRS (A) low q^2
MRST (98)
x
b)
$\bar{d}-\bar{u}$
GRV 94 LO, Q_0^2=54.0 GeV^2
HERMES $\langle Q^2 \rangle$=2.3 GeV^2
E866 Q^2=54.0 GeV^2
GRV 94 LO
$\langle Q^2 \rangle$=2.3 GeV^2
x

Possible explanations for $\bar{d}(x) > \bar{u}(x)$

- Pauli Blocking?

  The original assumption that $\bar{d}(x) = \bar{u}(x)$ comes from the idea that all sea quarks arise from the process $g \to q\bar{q}$, and since the u and d masses are equally small you don't expect a large asymmetry in their production. Perhaps, however, since $u(x) > d(x)$, then $g \to u\bar{u}$ might be suppressed relative to $g \to d\bar{d}$. But Ross and Sachrajda (Nucl. Phys. **B149** 497 (1979)) showed this is a small effect, on the order of 1%.

- Meson Cloud?

  The pions which "dress" a proton will produce additional anti-quarks in the environment. (Next slide)

- Chiral Perturbation Theory?

  Couplings between resident quarks and Goldstone bosons, in processes like $u \to d\pi^+$ and $d \to u\pi^-$, produce additional anti-quarks. Hence, since $u(x) > d(x)$, then there will be an excesss of $\bar{d}$ over $\bar{u}$ (excess of π^+ over π^-).

The origin of the nucleon sea is still under investigation! Additional experimental and theoretical work is needed.

Credit to the E866 publication J.C. Peng *et al.*, Phys. Rev. **D58** 092004 (1998), and references therein.

Much thanks to the E866 web page from which I shamelessly stole two of their very nice slides without permission.

Meson Cloud Models

- $|p\rangle = |p_0\rangle + a|N\pi\rangle + b|\Delta\pi\rangle$

$$\Rightarrow \text{ a: } |N\pi\rangle = \begin{cases} |p,\pi^0\rangle & \frac{u\bar{u}+d\bar{d}}{2} \\ |n,\pi^+\rangle & u\bar{d} \end{cases}$$

$$\Rightarrow \text{ b: } |\Delta\pi\rangle = \begin{cases} |\Delta^{++},\pi^-\rangle & d\bar{u} \\ |\Delta^{+},\pi^0\rangle & \frac{u\bar{u}+d\bar{d}}{2} \\ |\Delta^{0},\pi^+\rangle & u\bar{d} \end{cases}$$

- $\displaystyle\int_0^1 (\bar{d}-\bar{u})\,dx = \frac{1}{3}(2a-b) = 0.100 \pm 0.007 \pm 0.017$
  (NuSea)

- Recent calculations find $a \approx 2b$
  Phys. Rev. **D 53** (1996) 2586 and
  Nucl. Phys. **A 570** (1994) 765
  $\Rightarrow a = 2b = 0.20 \pm 0.036$

- $\displaystyle\frac{\bar{d}}{\bar{u}} = \frac{\frac{5}{6}a + \frac{1}{3}b + \text{pert. sea}}{\frac{1}{6}a + \frac{2}{3}b + \text{pert. sea}}$

Spin–Dependent Deep Inelastic Scattering

Two types of **inclusive** asymmetries will be measured at HERMES:

one for beam and target both polarized longitudinally ($A_\parallel$)

$$A_\parallel = \frac{\sigma^{\uparrow\downarrow} - \sigma^{\uparrow\uparrow}}{\sigma^{\uparrow\downarrow} + \sigma^{\uparrow\uparrow}}$$

and one for longitudinal beam and transverse target polarization ($A_\perp$)

$$A_\perp = \frac{\sigma^{\uparrow\rightarrow} - \sigma^{\uparrow\leftarrow}}{\sigma^{\uparrow\rightarrow} + \sigma^{\uparrow\leftarrow}}.$$

However, the physically more meaningful quantities are the asymmetries in virtual photon absorption, which are directly related to the structure functions:

$$A_1 = \frac{\sigma_{1/2} - \sigma_{3/2}}{\sigma_{1/2} + \sigma_{3/2}} = \frac{g_1 - \gamma^2 g_2}{F_1}$$

$$A_2 = \frac{\sigma_{TL}}{\sigma_T} = \frac{\gamma(g_1 + g_2)}{F_1}$$

where

$\sigma_{1/2} \quad \sigma_{3/2}$	virtual photon absorption cross sections
$\sigma_T = (\sigma_{1/2} + \sigma_{3/2})/2$	total transverse absorption cross section
σ_{TL}	transverse – longitudinal interference term
$g_1 \quad g_2$	spin – dependent structure functions
F_1	spin – independent structure function

Note that the kinematic factor $\gamma = \sqrt{Q^2}/\nu$ suppresses g_2 relative to g_1 in A_1. Also, it is anticipated theoretically, and found experimentally, that g_2 is small, nearly zero:

$$\Rightarrow \quad A_1 \approx \frac{g_1}{F_1}.$$

Spin–Dependent Deep Inelastic Scattering

The virtual photon absorption asymmetries are related to the experiment asymmetries:

$$\begin{aligned} A_{\parallel} &= D \cdot (A_1 + \eta \cdot A_2) \\ A_{\perp} &= d \cdot (A_2 - \xi \cdot A_1) \end{aligned}$$

where the kinematical factors D, d, η, and ξ are

$$\begin{aligned} D &= \frac{y(2-y)}{y^2 + 2(1-y)(1+R)} \\ \eta &= \frac{2\gamma(1-y)}{(2-y)} \\ d &= D\sqrt{\frac{2\epsilon}{1+\epsilon}} \\ \xi &= \eta\frac{1+\epsilon}{2\epsilon} \end{aligned}$$

and

$$\begin{aligned} \epsilon &= \frac{1-y}{1-y+y^2/2} \quad \text{(virtual photon polarization)} \\ R &= \sigma_L/\sigma_T \quad \text{(long./trans. cross section ratio)} \\ y &= \frac{\nu}{E} \quad \text{(fractional energy transfer to the nucleon).} \end{aligned}$$

Note that A_2 is suppressed in $A_{\parallel}$, and A_1 is suppressed in $A_{\perp}$:

$$\Rightarrow \quad A_{\parallel} \approx D \cdot A_1$$

$$\Rightarrow \quad A_{\perp} \approx d \cdot A_2$$

We noted already that $A_1 \approx g_1/F_1$:

$$\Rightarrow \quad A_{\parallel} \approx D\frac{g_1}{F_1}$$

This is a useful guide to thought.

HERMES Results from Inclusive Spin–Dependent Deep Inelastic Scattering

In 1995, a longitudinally polarized ^{3}He target was used at HERMES to study the spin structure of the neutron. The result for the polarized structure function $g_1^n(x)$ from this data has been published in K. Ackerstaff *et al.* (The HERMES Collaboration), Physics Letters **404B** 383 (1997). Our value for the integral of $g_1^n(x)$ over the range of our measurement is

$$\int_{0.023}^{0.6} g_1^n(x)dx = -0.034 \pm 0.013(\text{stat.}) \pm 0.005(\text{syst.})$$

at $\langle Q^2 \rangle = 2.5$ (GeV/c)^2. Extrapolating our data to $x = 0$ and $x = 1$, our value for the Ellis-Jaffe sum rule integral is

$$\Gamma_1^n = \int_0^1 g_1^n(x)dx = -0.037 \pm 0.013(\text{stat.}) \pm 0.005(\text{syst.}) \pm 0.006(\text{extrapol.}).$$

But beware: such extrapolations are fraught with assumptions about the behaviour of $g_1(x)$ as $x \to 0$ and $x \to 1$.

The most precise measure of $g_1^n(x)$ to date is that of the SLAC E154 Experiment, published in K. Abe *et al.* (The SLAC E154 Collaboration), Phys. Rev. Lett. **79** 26 (1997). Their value for the first moment of $g_1^n(x)$ over the range of their measurement is

$$\int_{0.023}^{0.7} g_1^n(x)dx = -0.036 \pm 0.004(\text{stat.}) \pm 0.005(\text{syst.})$$

at $\langle Q^2 \rangle = 5$ (GeV/c)^2.

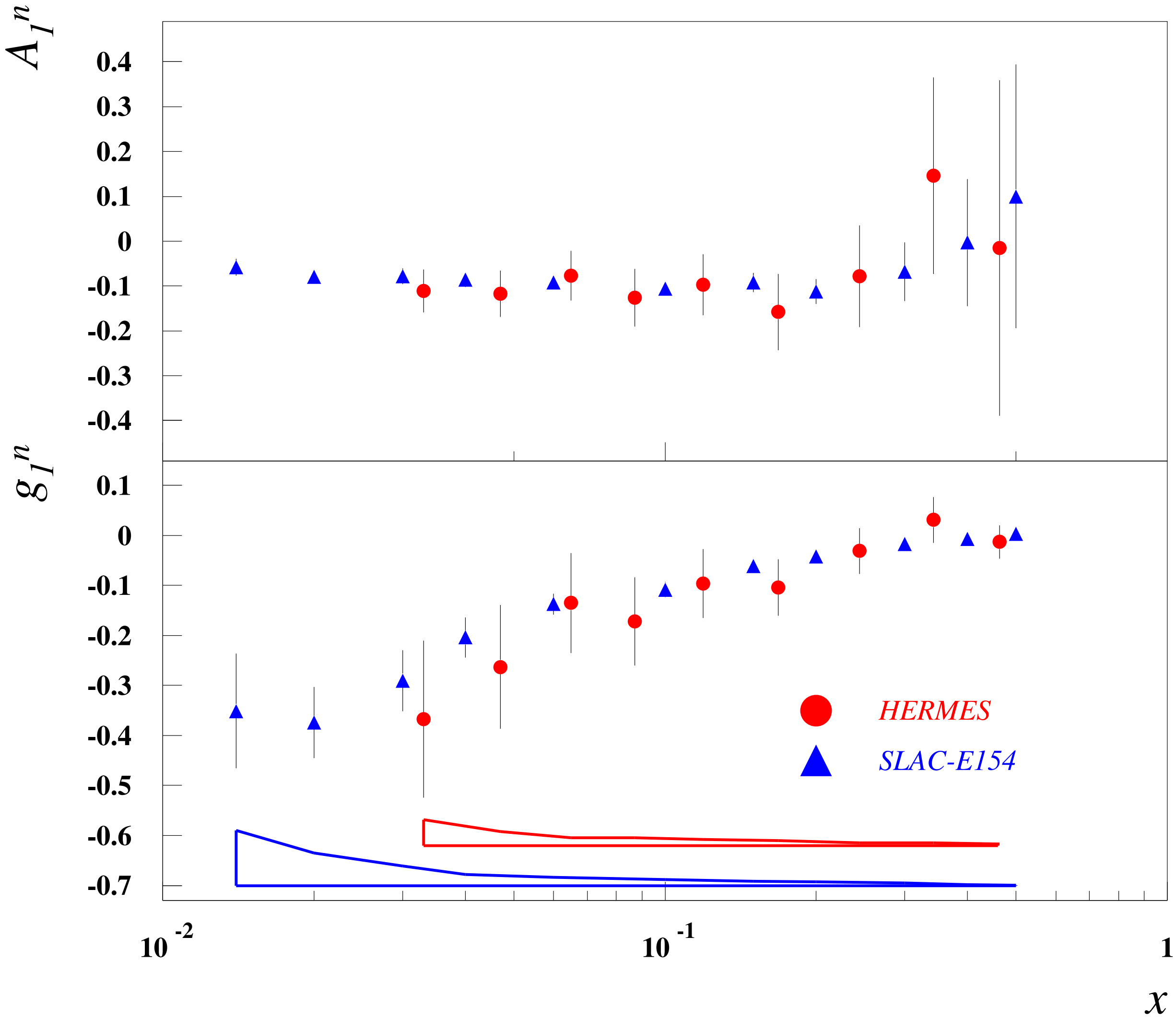

The structure function ratio $A_1^n = g_1^n/F_1^n$, and the structure function g_1^n of the neutron as a function of x, measured at HERMES and at SLAC (E-154). The error bars represent the statistical uncertainties while the error band represents the systematic uncertainties.

In 1996 and 1997 HERMES used a polarized ^{1}H target to study the spin structure of the proton. Our 1997 data for the polarized structure function $g_1^p(x)$ have been published in A. Airapetian *et al.*, (The HERMES Collaboration), Physics Letters **B442** 484 (1998).

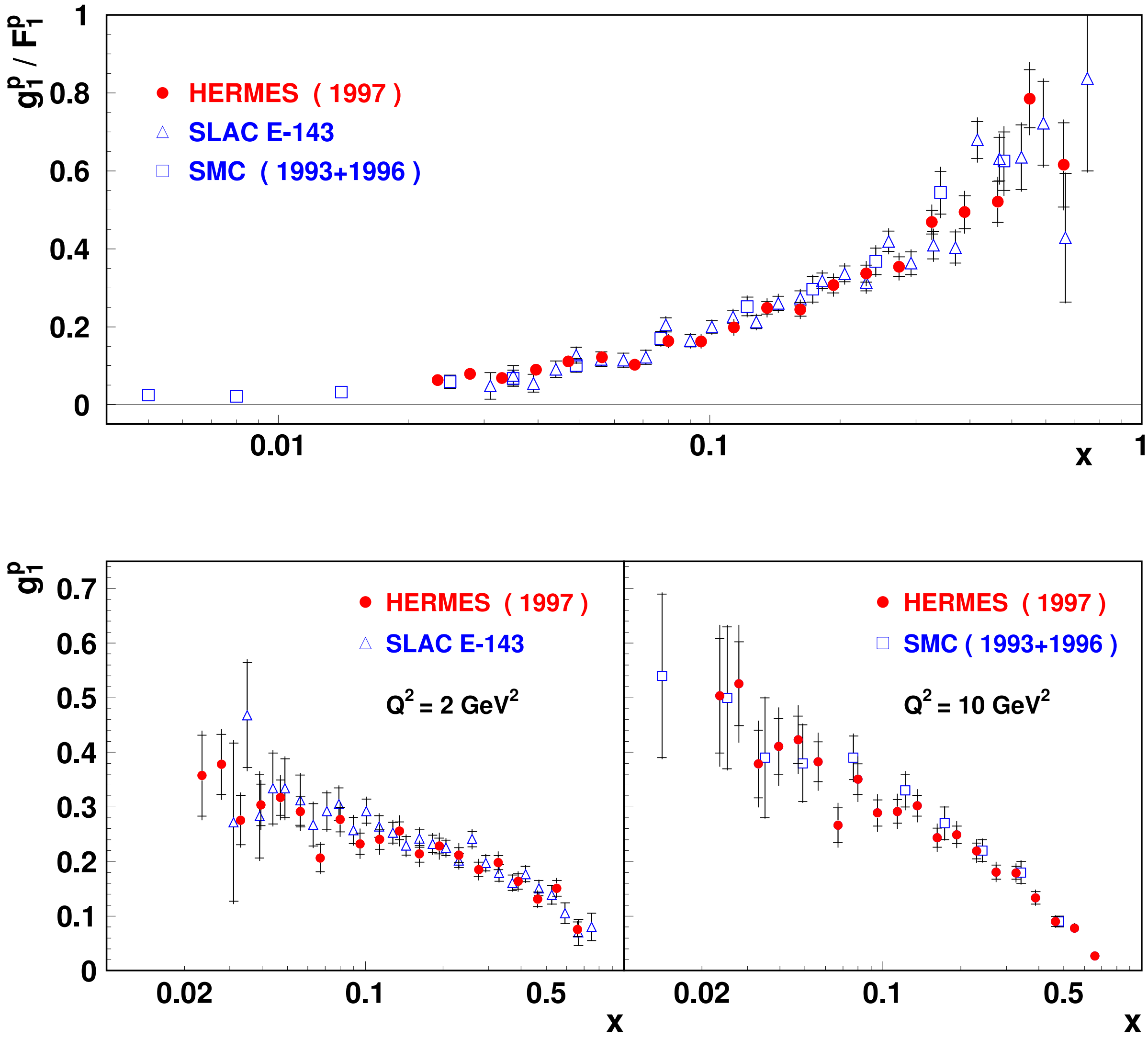

Top Panel: Comparison of HERMES data with recent results obtained at SLAC (E-143) and CERN (SMC). The inner error bars represent the statistical uncertainties and the outer ones the quadratic sum of the statistical and systematic uncertainties.

Bottom Panel: The spin structure function $g_1^p(x)$. The HERMES data are evolved to $Q_0^2 = 2$ (GeV/c)^2 (left) and $Q_0^2 = 10$ (GeV/c)^2 (right) assuming g_1/F_1 to be independent of Q^2. ALso shown are results for $Q^2 > 1$ (GeV/c)^2 from E-142 and from SLAC, the latter shown for $x > 0.01$ only.

Why is $|g_1^p(x)| >> |g_1^n(x)|$?

A **large cancelation** occurs in the neutron – even the naive quark model gets this right.

Recall

$$\int_0^1 g_1^p(x)dx = \frac{1}{2}\left(\frac{4}{9}\Delta u + \frac{1}{9}\Delta d + \frac{1}{9}\Delta s\right)$$

$$\int_0^1 g_1^n(x)dx = \frac{1}{2}\left(\frac{4}{9}\Delta d + \frac{1}{9}\Delta u + \frac{1}{9}\Delta s\right)$$

In the naive quark model, we saw that

$$\Delta u = 4/3 \qquad \Delta d = -1/3 \qquad \Delta s = 0$$

Then,

$$\begin{aligned}\int_0^1 g_1^p(x)dx &= \frac{1}{2}\left(\frac{4}{9}(4/3) + \frac{1}{9}(-1/3) + \frac{1}{9}(0)\right)\\ &= 5/18\end{aligned}$$

$$\begin{aligned}\int_0^1 g_1^n(x)dx &= \frac{1}{2}\left(\frac{4}{9}(-1/3) + \frac{1}{9}(4/3) + \frac{1}{9}(0)\right)\\ &= 0\end{aligned}$$

Semi-Inclusive Hadron Asymmetries

We consider the asymmetry in the yield of hadrons produced in deep-inelastic scattering:

$$A_{\|}^{h} = \frac{N_h^-(x) - N_h^+(x)}{N_h^-(x) + N_h^+(x)}$$

where N_h is the normalized yield of hadrons for a given beam-target helicity state (parallel or anti–paralell):

$$N_h(x,z) \propto \sum_f e_f^2 q_f(x) D_f^h(z)$$

We can relate $A_{\|}^{h}$ to a more fundamental asymmetry A_1^h similarly as in the case of inclusive scattering:

$$A_1^h \approx A_{\|}^{h}/D$$

where in terms of the quark–parton model,

$$A_1^h(x,Q^2,z) = \frac{\sum_f e_f^2 \Delta q_f(x,Q^2) D_f^h(x,Q^2)}{\sum_f e_f^2 q_f(x,Q^2) D_f^h(x,Q^2)} \frac{(1+R(x,Q^2))}{(1+\gamma^2)}.$$

For the purposes of the HERMES analysis, this expression is re-written thus:

$$A_1^h(x) = \sum_f P_f^h(x) \frac{\Delta q_f(x)}{q_f(x)} \frac{(1+R(x,Q^2))}{(1+\gamma^2)}$$

where

$$P_f^h(x) = \frac{e_f^2 q_f(x) \int_{0.2}^{1} D_f^h(z) dz}{\sum_{f'} e_{f'}^2 q_{f'}(x) \int_{0.2}^{1} D_{f'}^h(z') dz'}$$

are the integrated purities. We similarly express the inclusive asymmetry A_1 as

$$A_1(x) = \sum_f P_f(x) \frac{\Delta q_f(x)}{q_f(x)} \frac{(1+R(x,Q^2))}{(1+\gamma^2)}$$

where

$$P_f^h(x) = \frac{e_f^2 q_f(x)}{\sum_{f'} e_{f'}^2 q_{f'}(x)}.$$

Extraction of the Quark Polarizations $\frac{\Delta q}{q}(x)$

Altogether we can summarize these relations in a matrix form:

$$\vec{A}(x) = \mathbf{P}(x) \cdot \vec{Q}(x)$$

- the vector $\vec{A}(x) = \left(A_{1p}, A_{1p}^{h+}, A_{1p}^{h-}, A_{1He}, A_{1He}^{h+}, A_{1He}^{h-}\right)$ contains the measured inclusive and semi–inclusive asymmetries for the polarized hydrogen and helium targets
- the vector $\vec{Q}(x)$ contains the quark and anti–quark polarizations $\Delta q(x)/q(x)$
- the matrix operator $\mathbf{P}(x)$ contains the purities, indexed by type of measurement and quark flavor f, as well as the factor $(1 + R(x))/(1 + \gamma^2)$

The purities describe the probability that a virtual photon hit a quark of flavor f if a hadron of type h has been detected in the experiment. They are calculated in a Monte Carlo which includes

- the acceptance of the spectrometer
- a LUND string model for the fragmentation process
- parameterizations of the unpolarized quark distributions and for $R(x)$.

The fragmentation functions for the sea quarks are much smaller than for the valence quarks, producing an unstable numerical situation if you try to extract all six u, d, and s polarized distribution functions — some additional constaints must be placed on these functions in order to extract a result. Several choices for these constraints are possible! In the system presented here, we make a distinction between the valence and sea contributions of the u quarks

$$u(x) \equiv u_v(x) + u_s(x) \qquad u_s(x) \equiv \bar{u}(x)$$

and similarly for the d quarks. Then, we seek to obtain a solution for the vector

$$\vec{Q}(x) = \left(\frac{(\Delta u + \Delta\bar{u})}{(u + \bar{u})}(x), \frac{(\Delta d + \Delta\bar{d})}{(d + \bar{d})}(x), \frac{(\Delta s + \Delta\bar{s})}{(s + \bar{s})}(x)\right)$$

with the requirement that all sea quarks have the **same polarization:**

$$\frac{\Delta q_s}{q_s}(x) \equiv \frac{\Delta u_s}{u_s}(x) = \frac{\Delta d_s}{d_s}(x) = \frac{\Delta s}{s}(x) = \frac{\Delta\bar{u}}{\bar{u}}(x) = \frac{\Delta\bar{d}}{\bar{d}}(x) = \frac{\Delta\bar{s}}{\bar{s}}(x)$$

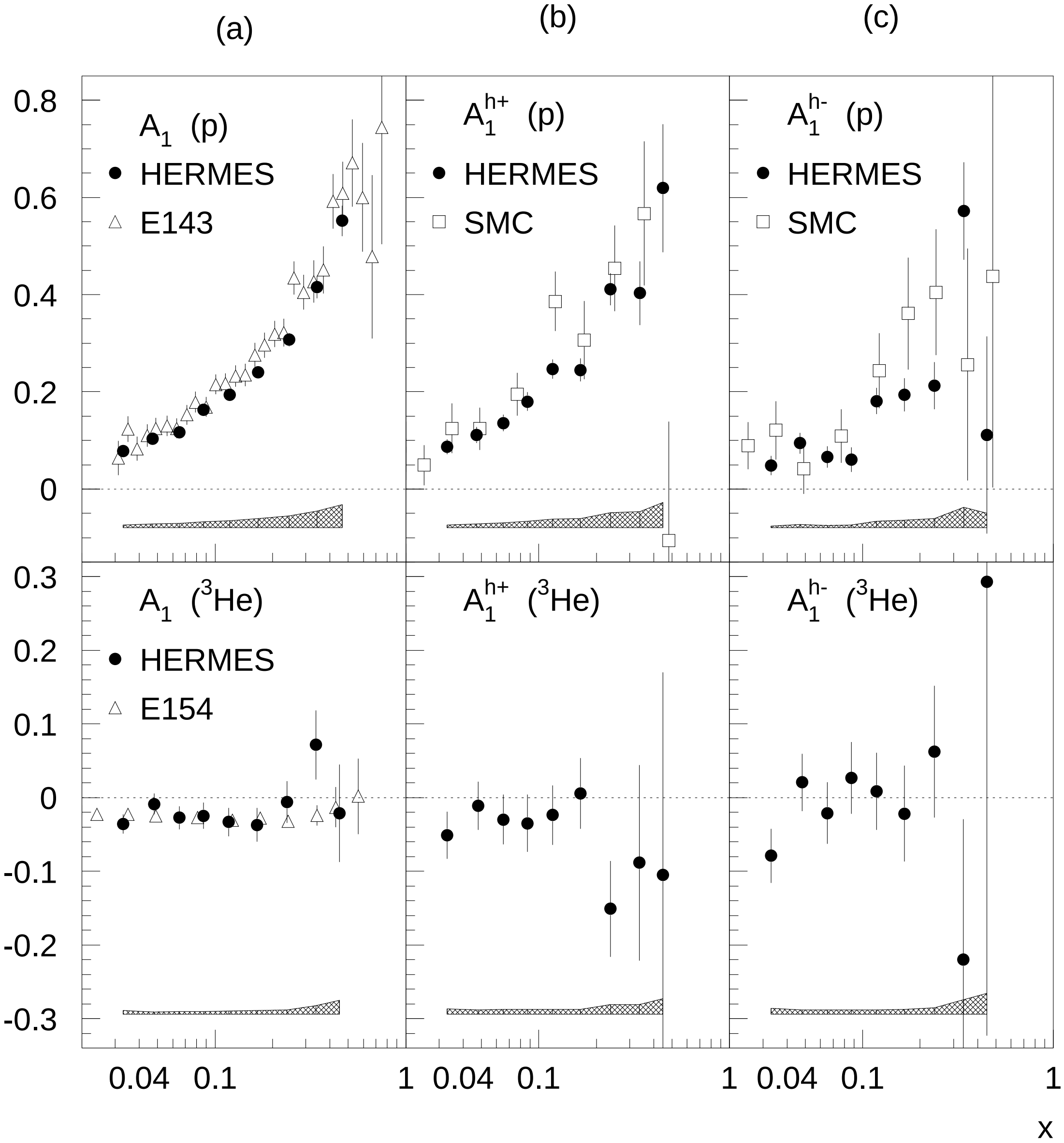

Asymmetries from which the quark polarizations are extracted. Inclusive (a) and semi–inclusive asymmetries for positive (b) and negative (c) hadrons are shown. The inclusive asymmetries are compared to the SLAC results for g_1/F_1 (open triangles). The semi–inclusive asymmetries are compared to the SMC results for the proton (open squares), truncated to the HERMES x-range. Error bars for HERMES are statistical only, while those of SLAC and SMC are total uncertainties. The error bands are the systematic uncertainties for HERMES.

No effort has been made to correct any data for the considerable differences in Q^2 in the various experiments.

HERMES Results for the Quark Polarizations $\frac{\Delta q}{q}(x)$

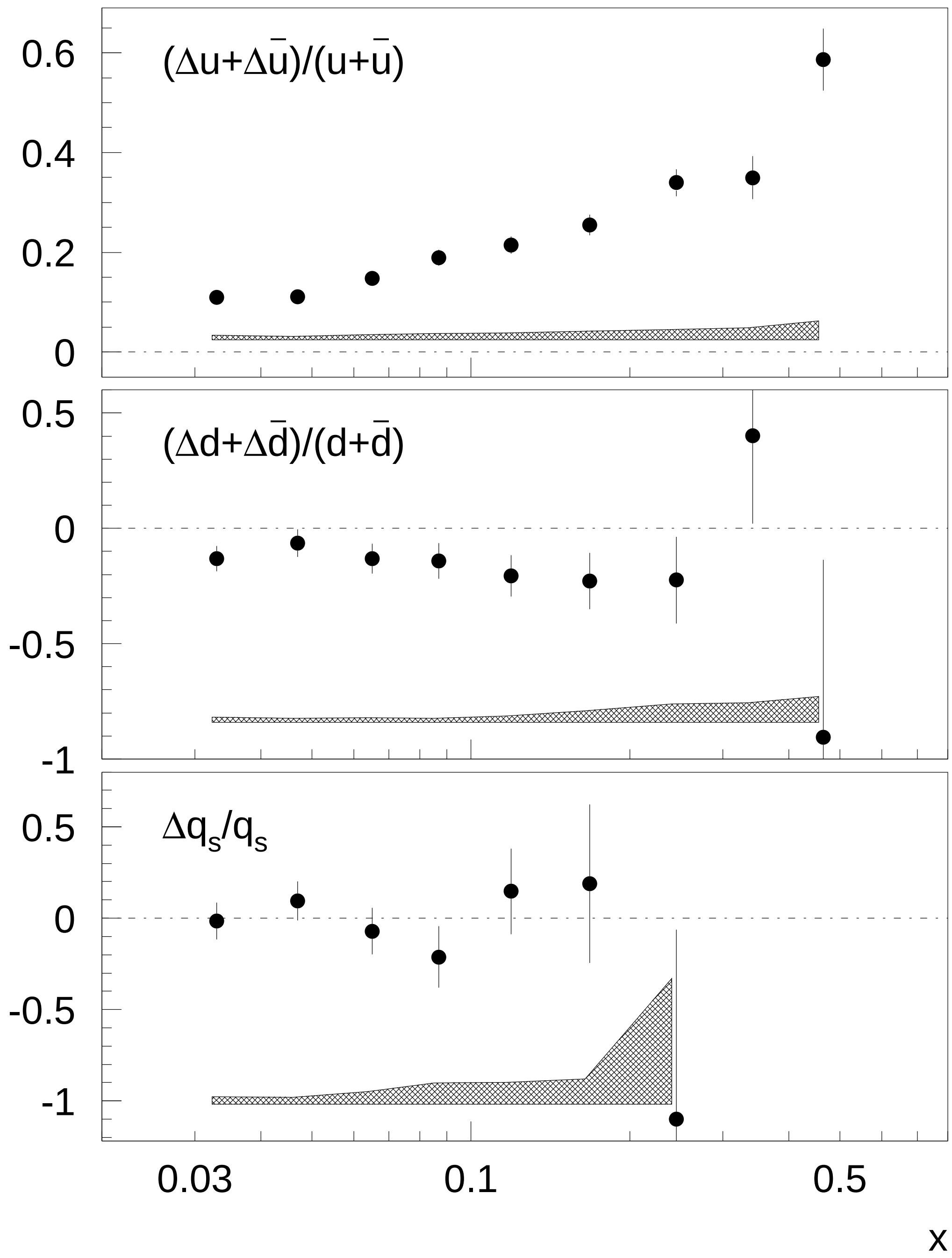

The flavor decomposition of the quark polarization as a function of x, derived from the HERMES inclusive and semi–inclusive asymmetries, assuming a flavor symmetric sea polarization. Error bars are statistical; error bands are systematic.

Discussion of Quark Polarization Results

- Strange quark polarization – conflict? Recall that by assuming SU(3)–flavor symmetry, we were able to use the F and D coefficients from β-decay and an inclusive measurement of $g_1^p(x)$ to get the moments Δu, Δd, and Δs, and we found a significant negative Δs. Our new results, which assumed a asymmetric sea polarization, give an unpolarized sea. But these two results are each bound by their own (and different) assumptions, and **neither is a direct measure of the strange quark polarization** – this will have to wait (see later slides).

- Non-singlet contribution — In the quark-parton model, the combination

$$\Delta q^{NS}(x) = \Delta u(x) + \Delta \bar{u}(x) - \Delta d(x) - \Delta \bar{d}(x)$$

is related directly to the proton and neutron spin structure functions by

$$\Delta q^{NS}(x) = 6(g_1^p(x) - g_1^n(x)).$$

Our results for this combination from our data can be compared to parametrizations of other world inclusive data, with which they are in agreement (see the slide). The integral of the non-singlet contribution is related to the fundamental Bjorken sum-rule

$$\int_0^1 (g_1^p(x) - g_1^n(x))dx = |g_a/g_v| \cdot (\text{QCD corrections})$$

and our value is consistent with the theoretical one.

- Try another assumption about the sea? Instead of a sea polarization independent of flavor, we can instead assume a singlet spin distribution for the sea:

$$\Delta q_s(x) \equiv \Delta u_s(x) = \Delta d_s(x) = \Delta s(x) = \Delta \bar{u}(x) = \Delta \bar{d}(x) = \Delta \bar{s}(x)$$

The results for the quark polarizations are essentially the same (see the slide). This result also implies that we are not yet sensitive enough to test the validity of flavor–SU(3) symmetry. This again will require a direct measurement of the strange quark polarization.

Non-singlet Contribution

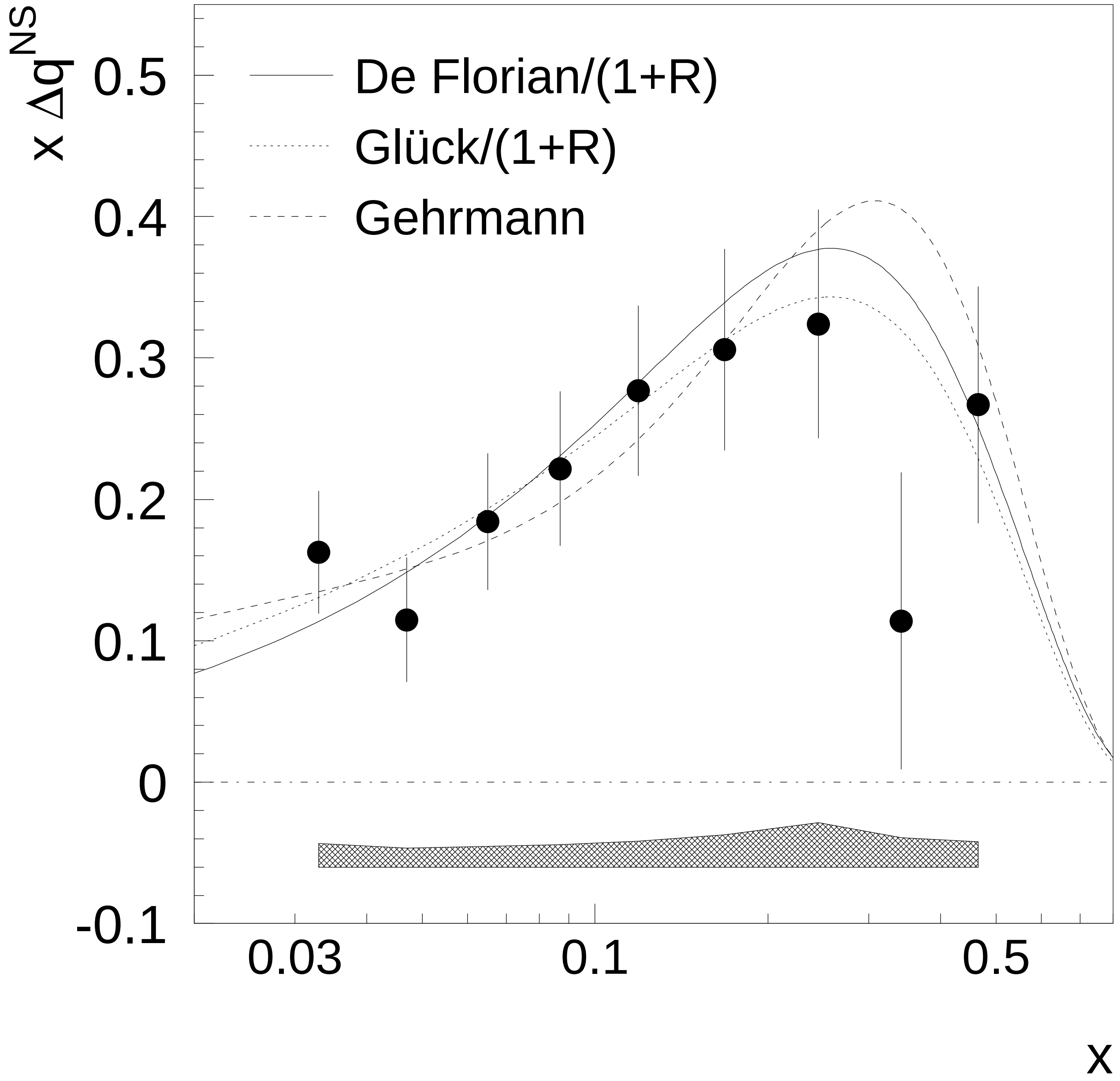

The non-singlet contribution

$$x\Delta q_{NS}(x) = x(\Delta u(x) + \Delta\bar{u}(x) - \Delta d(x) - \Delta\bar{d}(x))$$

at $Q^2 = 2.5$ GeV^2. The result is compared to parametrizations derived from inclusive data from other experiments. Error bars are statistical, error bands are systematic.

Flavor-Independent Sea Polarization vs. Singlet Sea Spin Distribution

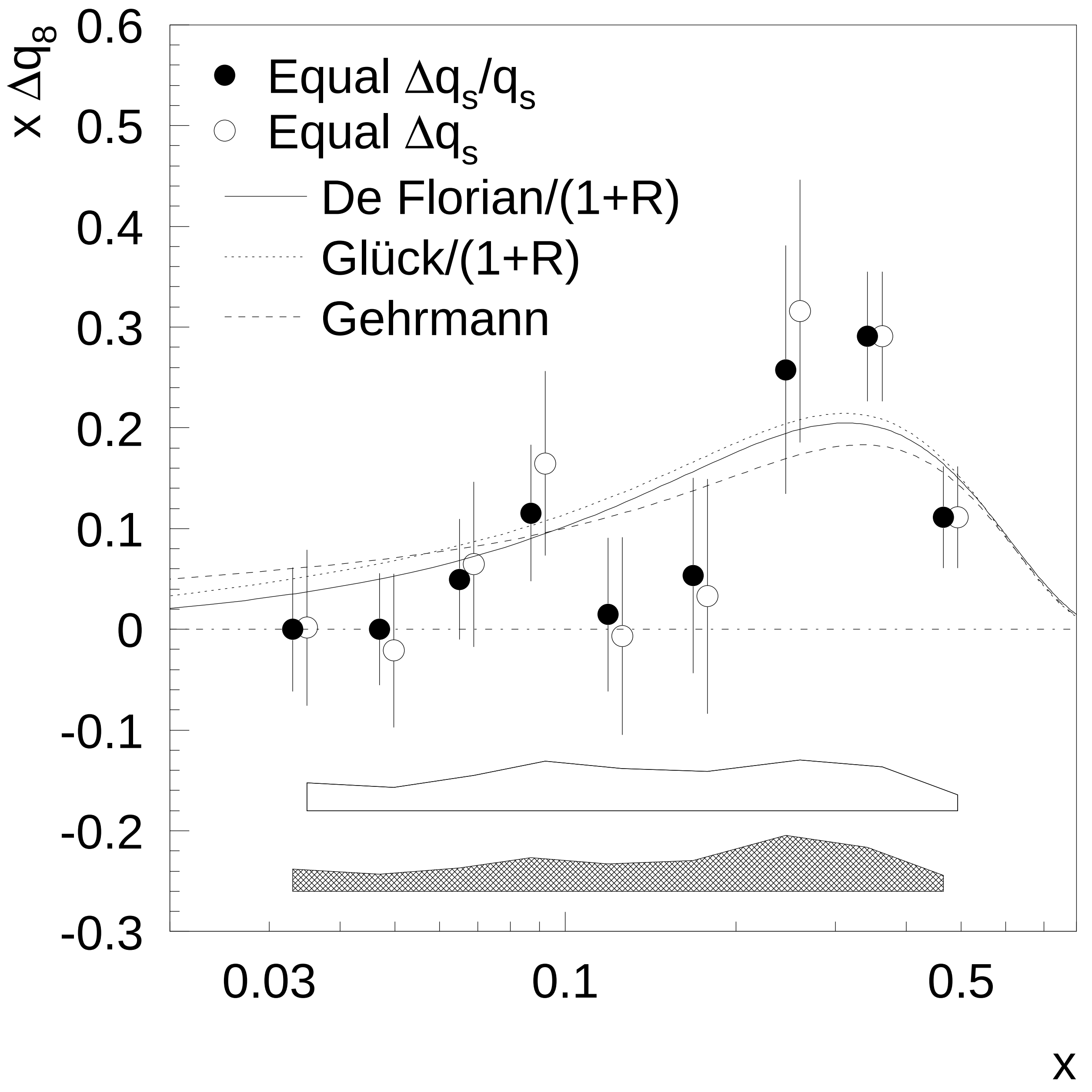

The SU(3)–flavor octet combination

$$x\Delta q_8(x) = x(\Delta u(x) + \Delta\bar{u}(x) + \Delta d(x) + \Delta\bar{d}(x) - 2(\Delta s(x) + \Delta\bar{s}(x)))$$

at $Q^2 = 2.5\ \mathrm{GeV}^2$. The result is compared to parametrizations derived from inclusive data from other experiments. Error bars are statistical, error bands are systematic. The closed circles assume the flavor-independent sea polarization, while the open circles assume a singlet sea spin distribution – the results are essentially identical.

The RICH Detector allows a measurment of the Strange Quark Polarization $\frac{\Delta s}{s}(x)$

Until 1998, HERMES was restricted to the observation of leptons, pions, and heavier unidentified hadrons. [In certain limited kinematic regimes, heavier particles such as kaons and protons could be identified.] With the introduction of the RICH detector, now charged kaons and also protons can be identified in each event over a broad kinematic range. The observation of the asymmetry in the semi–inclusive production of K^+ and K^- gives us a stronger handle on the strange quark polarization in the nucleon.

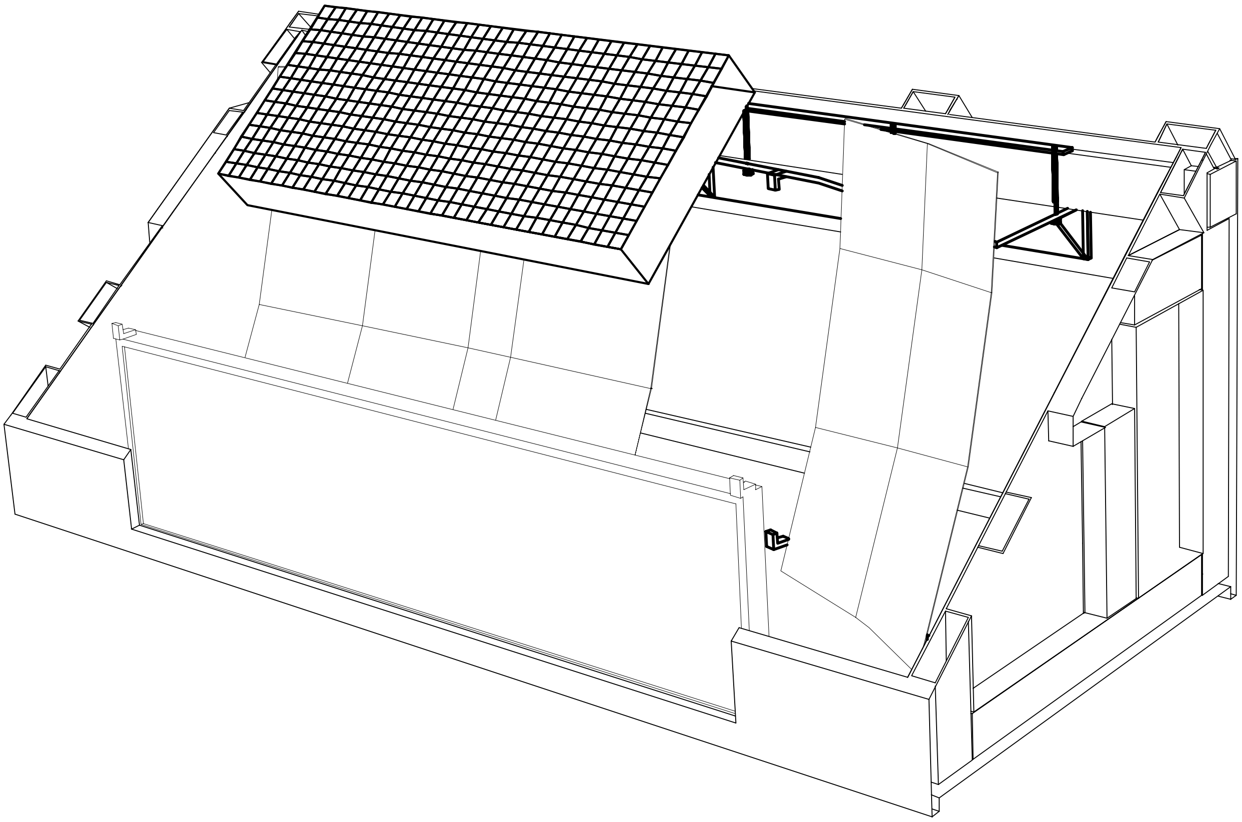

A cutaway schematic view of the RICH counter. The entrance region is covered by a place of Aerogel 5cm thick. A section of the spherical mirror has been cut away for display purposes. The photon detector is indicated by the canted rectangular volume above the sensitive region.

The Strange Future of HERMES

Preliminary HERMES results for the valence and sea quark polarizations covering the data from 1995-1997 (which we present here for statistical comparison only), and the expectation for the uncertainties after two more years of data with the RICH detector and a polarized deuterium target.

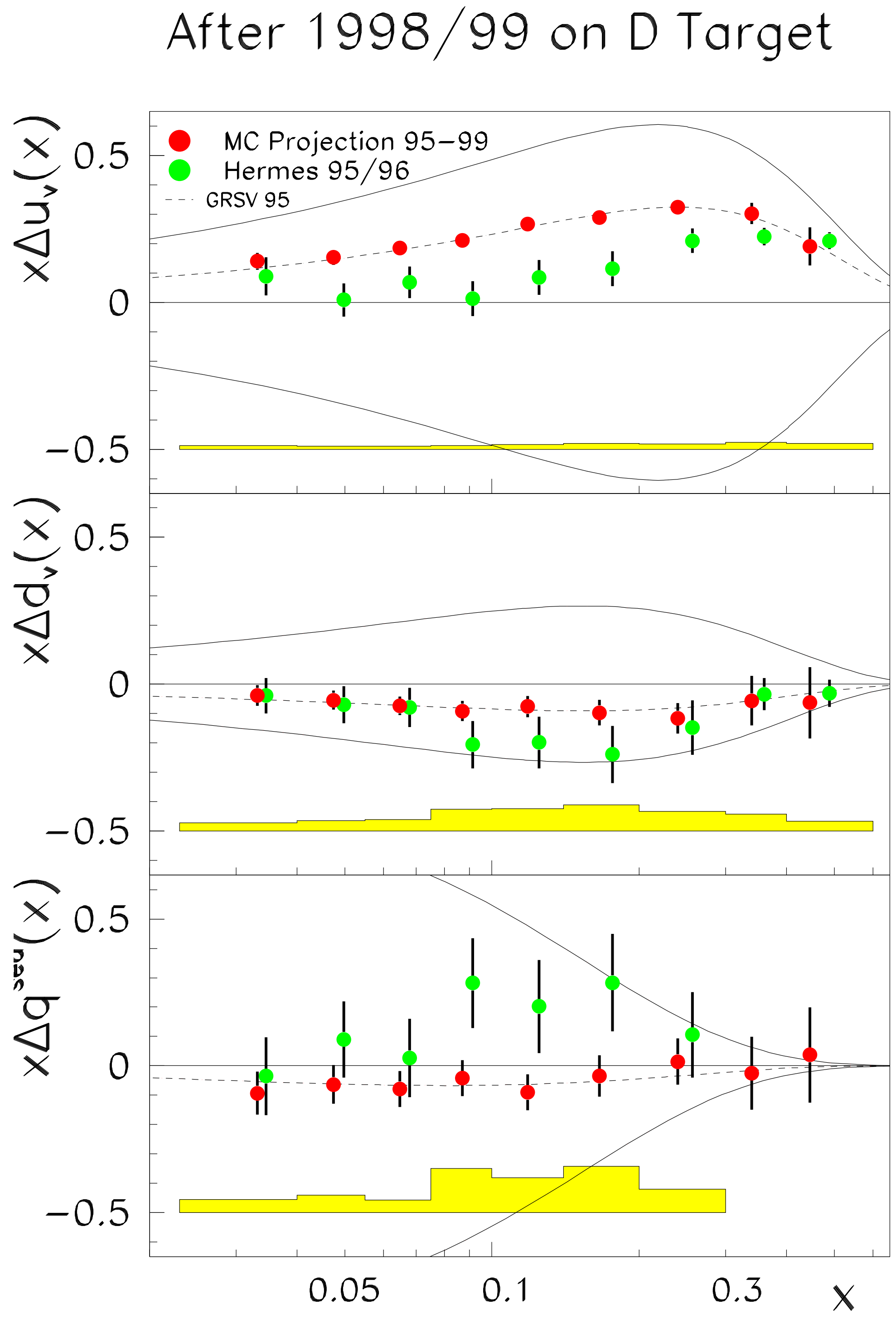

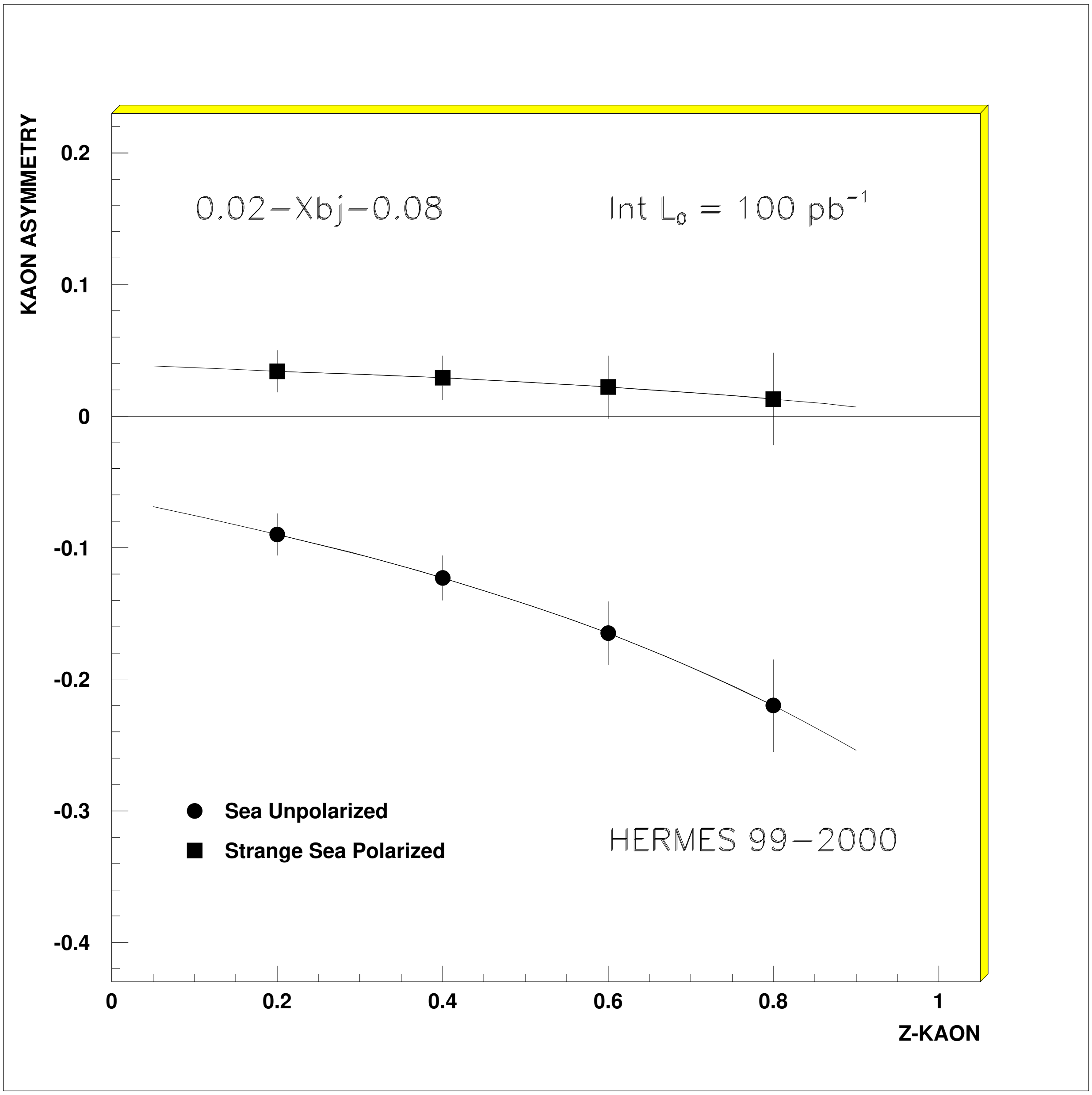

Results of a Monte Carlo simulation of $A^{K^-}(z)$ for an unpolarized sea, and for a maximally negatively polarized strange sea ($\Delta\bar{q} = 0, \Delta\bar{s} = -\bar{s}$), with $0.02 \leq x_{BJ} \leq 0.08$. The error bars indicate the statistical precision with which $A_p^{K^-}(z)$ would be measured in HERMES using a polarized deuterium target in two years of normal running (two "standard runs").

The Spin of the Λ

The Λ is the lightest strange baryon: a uds quark state. In hadronic interactions, it is always produced in associated with a strange meson, typically a kaon. The Λ has a spin of 1/2, while the kaon is spinless.

The Λ primarily decays *via* the weak neutral current channel:

$$\Lambda \to p\pi^-$$

As this decay is parity-violating, it will display an angular distribution with respect to the spin axis of the Λ:

$$dN \propto (1 + \beta P_\Lambda \cos\Theta_{p\Lambda})d\Omega$$

where

$$\beta = 0.642 \pm 0.013 \quad \text{asymmetry parameter}$$

$$P_\Lambda \quad \Lambda \text{ polarization}$$

$$\Theta_{p\Lambda} \quad p - \Lambda \text{ angle in } \Lambda \text{ c.m.}$$

Hence, the detection of the Λ through the $\Lambda \to p\pi^-$ channel includes information about its polarization.

In the naive quark model, the spin of the Λ is carried by the s-quark:

$$\begin{aligned}|\Phi_\Lambda> = \frac{1}{\sqrt{12}}|&u{\uparrow}d{\downarrow}s{\uparrow} - u{\downarrow}d{\uparrow}s{\uparrow} - d{\uparrow}u{\downarrow}s{\uparrow} + d{\downarrow}u{\uparrow}s{\uparrow}\\ &+ d{\downarrow}s{\uparrow}u{\uparrow} - d{\uparrow}s{\uparrow}u{\downarrow} - u{\downarrow}s{\uparrow}d{\uparrow} + u{\uparrow}s{\uparrow}d{\downarrow}\\ &+ s{\uparrow}u{\uparrow}d{\downarrow} - s{\uparrow}u{\downarrow}d{\uparrow} - s{\uparrow}d{\uparrow}u{\downarrow} + s{\uparrow}d{\downarrow}u{\uparrow}>\end{aligned}$$

so that

$$\Delta u = 0 \qquad \Delta d = 0 \qquad \Delta s = 1.$$

Polarization of Λ's produced in DIS

However... some facts to consider.

- The polarization of the Λ is not entirely due to its s-quark: The same naive quark model which is wrong for the nucleon is also wrong for the Λ.
- HERMES has significant acceptance for the production of Λ's through *current* fragmentation only: Within the present detector configuration, those produced in *target* fragmentation tend not to decay into the detector acceptance.
- It is tempting to consider the fragmentation of struck s-quarks into Λ's as a source of information about the polarization of s-quarks in the nucleon, but in fact u-quarks are much more probably found in the nucleon than are s-quarks and the interaction rate in DIS is higher by the ratio $(e_u/e_s)^2 = 4$.
- Not only the Λ but also the Σ^0 can be produced in DIS, and the $\Sigma^0 \to \Lambda\gamma$ decay will contribute to the production of Λ's. Since this decay can have a significant spin-flip amplitude, any measurement of Λ polarization must be corrected for Σ^0 production.
- To the extent that Flavor–SU(3) is a good symmetry, then values of moments like Δu, *etc*... in the proton will be related to those same moments in the Λ.

u-quark dominance of Λ production in DIS

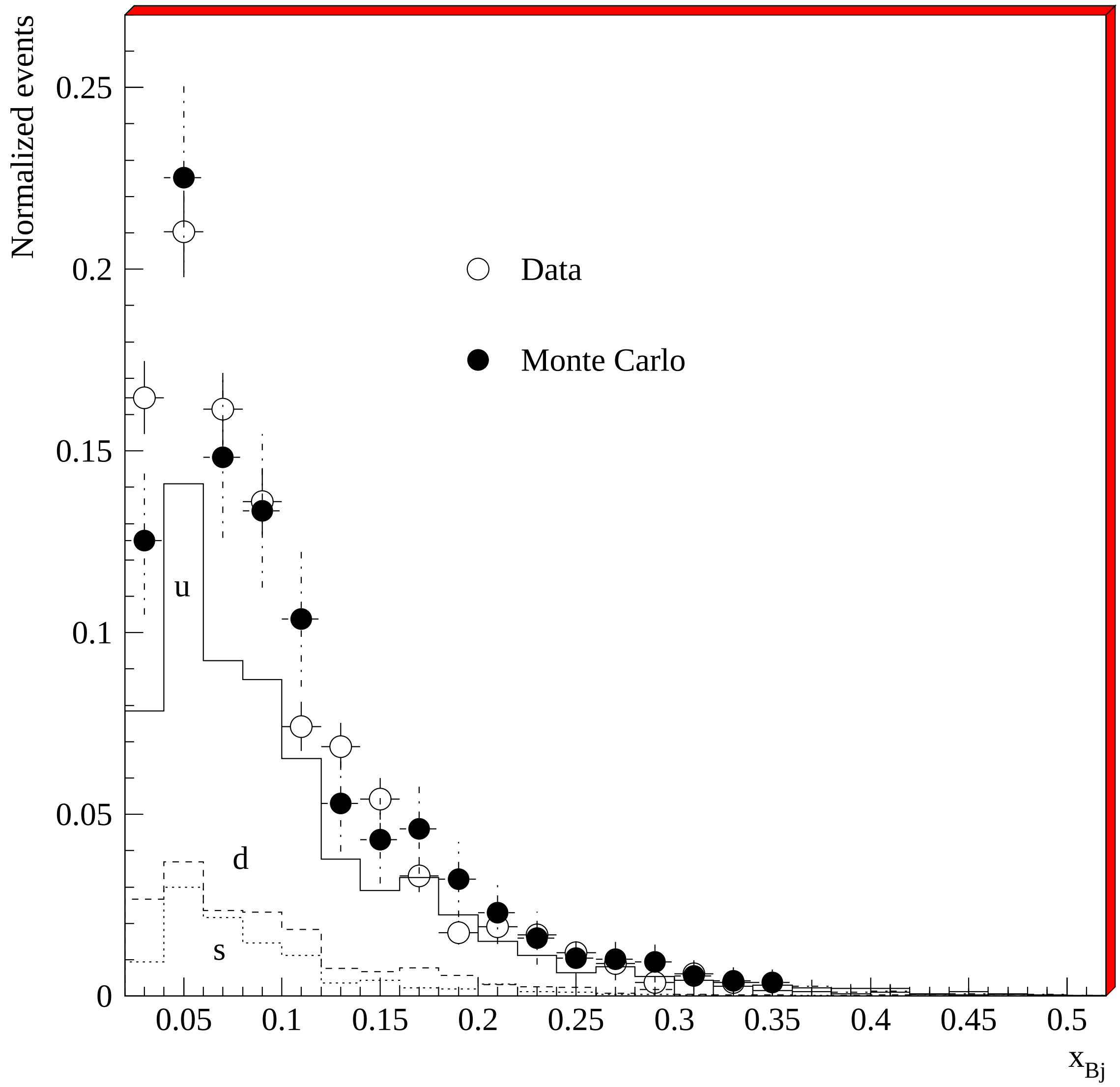

Taking into account not only the ratio of quark charges but also the distribution functions, a Monte Carlo simulation of the production and detection of Λ's from a proton target in HERMES shows the dominance of the u-quark in this process even down to low x_{BJ}.

Polarized Fragmentation

In the case of a longitudinally polarized electron beam and an *unpolarized* hydrogen target, the polarization of the Λ is

$$\vec{P}_\Lambda = \hat{e}_3 P_e \frac{y(2-y)}{1+(1-y)^2} \frac{\sum_f e_f^2 q_f^N(x,Q^2)\Delta D_f^\Lambda(z,Q^2)}{\sum_f e_f^2 q_f^N(x,Q^2) D_f^\Lambda(z,Q^2)},$$

or

$$P_\Lambda = P_e D(y) D_{LL'}^\Lambda$$

where P_e is the beam polarization, the Λ–momentum defines the $\hat{e}_3$ axis, $D(y) = \frac{y(2-y)}{1+(1-y)^2}$, and the spin transfer coefficient $D_{LL'}^\Lambda$ contains all the information concerning the transfer of the quark spin to the Λ during fragmentation:

$$D_{LL'}^\Lambda = \frac{\sum_f e_f^2 q_f^N(x,Q^2)\Delta D_f^\Lambda(z,Q^2)}{\sum_f e_f^2 q_f^N(x,Q^2) D_f^\Lambda(z,Q^2)}$$

Taking the notion that the u-quarks dominate the process to the limit, this reduces to

$$D_{LL'}^\Lambda = \frac{\Delta D_u^\Lambda(z,Q^2)}{D_u^\Lambda(z,Q^2)},$$

so that

$$\vec{P}_\Lambda = \hat{e}_3 P_e D(y) \frac{\Delta D_u^\Lambda(z,Q^2)}{D_u^\Lambda(z,Q^2)}.$$

For typical HERMES conditions this gives

$$P_\Lambda \sim 0.3 \frac{\Delta D_u^\Lambda(z,Q^2)}{D_u^\Lambda(z,Q^2)}.$$

If a significant Λ polarization is observed, then it most likely arises from the u-quarks and confirms the notion of significant u-quark polarization in the Λ.

Extraction of Λ Polarization and $D_{LL'}^{\Lambda}$

The parity–violating decay $\Lambda \to p\pi^-$ produces an angular distribution of the decay products according to the polarization of the Λ along its direction of motion:

$$N_\Lambda \propto (1 + 0.642 \cdot P_\Lambda \cos(\Theta_{p\Lambda}))$$

Analysis of this angular distribution under reversal of the beam helicity permits extraction of P_Λ and hence the spin–transfer factor $D_{LL'}^{\Lambda}$.

Our present data set includes runs with unpolarized hydrogen and deuterium gases during 1996 and 1997. The beam helicity was positive in 1996 and negative in 1997 — not an example of rapid spin reversal!

Selecting a data sample for which the luminosity–weighted average beam polarization is *zero* (*i.e.*, including really equal amounts of data from each beam helicity state), and assuming that the detector acceptance is constant, the spin transfer to the Λ can be related to the asymmetry in Λ production by

$$D_{LL'}^{\Lambda} = \frac{\left(\Sigma_{i=1}^{N_\Lambda} P_{B,i} \cos\Theta_{p\Lambda,i}\right)}{\left(\beta ||P_B^2|| \, \Sigma_{i=1}^{N_\Lambda} D(y_i) \cos^2\Theta_{p\Lambda,i}\right)}$$

where the sum is over the Λ events in the dataset, and $||P_B^2||$ is the luminosity-weighted average square of the beam polarization. This expression cancels out any asymmetry in the detector acceptance.

Preliminary HERMES results for Longitudinal Λ polarization in the current fragmentation region

$$< z > \ = \ 0.5$$

$$< Q^2 > \ = \ 2.5\text{GeV}^2$$

$$D_{LL'}^{\Lambda} \ = \ 0.10 \pm 0.17 \pm 0.09(\text{syst})$$

$$P_{\Lambda} \ = \ 0.03 \pm 0.06 \pm 0.03(\text{syst})$$

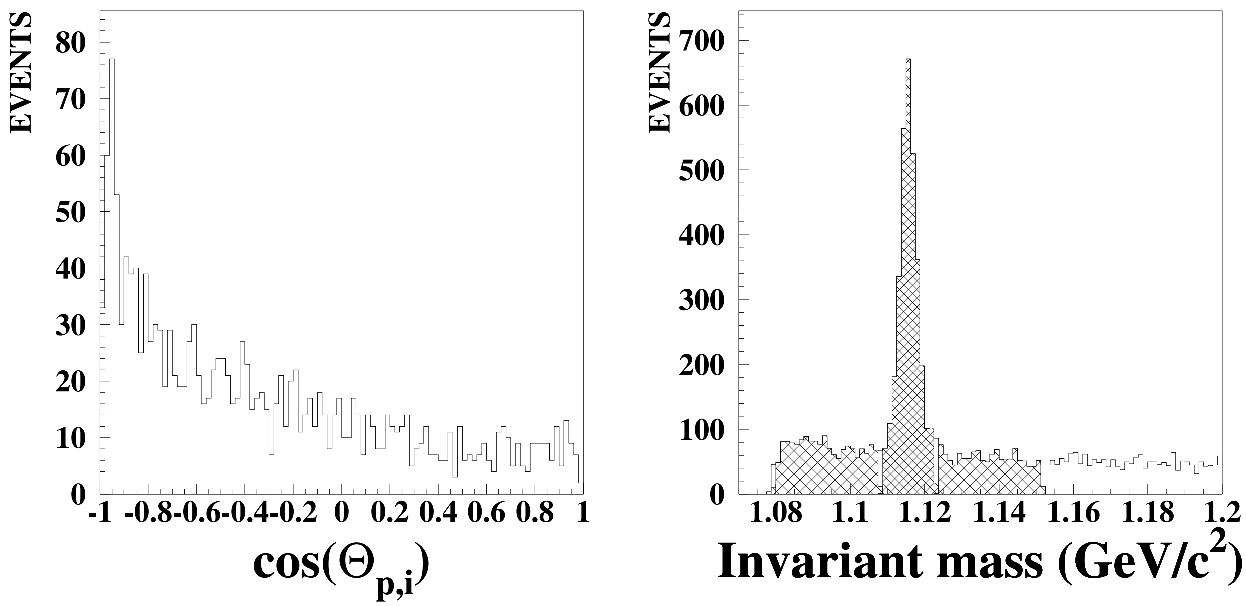

Left: Spectrum of $\cos\Theta_{p\Lambda,i}$. Most of the apparent asymmetry in the $\cos\Theta_{p\Lambda,i}$ spectrum is due to the asymmetric acceptance of the spectrometer for these events.

Right: Spectrum of $p\pi^-$ invariant mass, in the region of the Λ. The shaded regions to the left and right of the Λ mass peak are used for background analysis.

Remember SU(3)?

Recall that by assuming flavor–SU(3) symmetry, we can calculate the moments Δu, Δd, and Δs for the proton by using the values of the F and D coefficients from β-decay and a measurement of $g_1^p(x)$ from inclusive DIS:

$$\begin{aligned} a_0 &= \Delta u + \Delta d + \Delta s \\ &\equiv \Delta\Sigma \text{ (quark contribution to proton spin)} \\ a_3 &= \Delta u - \Delta d \\ a_8 &= \frac{1}{\sqrt{3}} (\Delta u + \Delta d - 2\Delta s) \end{aligned}$$

combined with

$$\int_0^1 g_1^p(x)dx = \frac{1}{12}\left(a_3 + \frac{1}{\sqrt{3}}a_8 + \frac{4}{3}a_0\right)$$

and

$$\begin{aligned} a_3 &= D + F \\ a_8 &= \frac{1}{\sqrt{3}}(3F - D). \end{aligned}$$

where F and D are

$$F = 0.477 \pm 0.012 \qquad D = 0.756 \pm 0.011$$

finally yields (as it is usually written):

$$\begin{aligned} \Delta u^p &= (\Delta\Sigma + D + 3F)/3 \\ \Delta d^p &= (\Delta\Sigma - 2D)/3 \\ \Delta s^p &= (\Delta\Sigma + D - 3F)/3 \end{aligned}$$

where I have attached an explicit "proton" label to these values. Then, as we have already seen,

$$\begin{aligned} \Delta u^p &= +0.79 \pm 0.04 \\ \Delta d^p &= -0.45 \pm 0.04 \\ \Delta s^p &= -0.16 \pm 0.04. \end{aligned}$$

The Proton, the Λ, and Flavor SU(3)

Flavor–SU(3) symmetry additionally allows you to relate these moments among all the members of the SU(3) baryon octet (Schnell and Burkardt):

	Δu	Δd	Δs
p	$\frac{1}{3}(\Delta\Sigma + D + 3F)$	$\frac{1}{3}(\Delta\Sigma - 2D)$	$\frac{1}{3}(\Delta\Sigma + D - 3F)$
n	$\frac{1}{3}(\Delta\Sigma - 2D)$	$\frac{1}{3}(\Delta\Sigma + D + 3F)$	$\frac{1}{3}(\Delta\Sigma + D - 3F)$
Σ^+	$\frac{1}{3}(\Delta\Sigma + D + 3F)$	$\frac{1}{3}(\Delta\Sigma + D - 3F)$	$\frac{1}{3}(\Delta\Sigma - 2D)$
Σ^0	$\frac{1}{3}(\Delta\Sigma + D)$	$\frac{1}{3}(\Delta\Sigma + D)$	$\frac{1}{3}(\Delta\Sigma - 2D)$
Σ^-	$\frac{1}{3}(\Delta\Sigma + D - 3F)$	$\frac{1}{3}(\Delta\Sigma + D + 3F)$	$\frac{1}{3}(\Delta\Sigma - 2D)$
Λ	$\frac{1}{3}(\Delta\Sigma - D)$	$\frac{1}{3}(\Delta\Sigma - D)$	$\frac{1}{3}(\Delta\Sigma + 2D)$
Ξ^0	$\frac{1}{3}(\Delta\Sigma - 2D)$	$\frac{1}{3}(\Delta\Sigma + D - 3F)$	$\frac{1}{3}(\Delta\Sigma + D + 3F)$
Ξ^-	$\frac{1}{3}(\Delta\Sigma + D - 3F)$	$\frac{1}{3}(\Delta\Sigma - 2D)$	$\frac{1}{3}(\Delta\Sigma + D + 3F)$

So that the measurement of F, D, and $g_1^p(x)$ predicts for the entire baryon octet:

	Δu	Δd	Δs
p	0.79 ± 0.04	-0.45 ± 0.04	-0.16 ± 0.05
n	-0.45 ± 0.04	0.79 ± 0.04	-0.16 ± 0.05
Σ^+	0.79 ± 0.04	-0.16 ± 0.05	-0.45 ± 0.04
Σ^0	0.32 ± 0.04	0.32 ± 0.04	-0.45 ± 0.04
Σ^-	-0.16 ± 0.05	0.79 ± 0.04	-0.45 ± 0.04
Λ	-0.20 ± 0.04	-0.20 ± 0.04	0.58 ± 0.04
Ξ^0	-0.45 ± 0.04	-0.16 ± 0.05	0.79 ± 0.04
Ξ^-	-0.16 ± 0.05	-0.45 ± 0.04	0.79 ± 0.04

So, in particular for the Λ, we see that the current data (assuming flavor–SU(3) is valid) predicts a very significant -0.20 contribution from the u and d quarks to the overall spin.

Flavor–SU(3) and Fragmentation

Significantly, it turns out that the moments of the polarized fragmentation functions, *i.e.*

$$\Delta D_f^\Lambda \equiv \int_o^1 \Delta D_f^\Lambda(z)dz$$

obey the same algebra as the moments of the polarized quark distribution functions. In this context, we place a "carat" over the (unknown) parameters of that algebra:

$$\hat{\Delta\Sigma} \qquad \hat{F} \qquad \hat{D}.$$

So, for example,

$$\Delta D_u^\Lambda = \left(\hat{\Delta\Sigma} - \hat{D}\right)/3.$$

We can learn about these parameters by comparing the results of the HERMES deep-inelastic polarized Λ production and that done *via* the Z^0–pole at ALEPH.

(thanks to M. Burkardt and G. Schnell for much of the following discussion)

ALEPH

- e^+e^- at Z^0-pole
- use $e^+e^- \longrightarrow \Lambda + X$ to learn about $q \longrightarrow \Lambda$ fragmentation
- parity violating e^-Z^0 and qZ^0 couplings
  $\hookrightarrow$ produces "polarized quark beam"
- parity violating decay of Λ self-analysing
  $\hookrightarrow$ polarized $q \longrightarrow \Lambda$ fragmentation functions
- "beam composition":

$$u_L - u_R + d_L - d_R \;:\; s_L - s_R \;=\; 61\% \;:\; 39\%$$

  $\hookrightarrow$ nearly flavor singlet: measures $\hat{\Delta\Sigma} + .16\hat{D}$
  $\hookrightarrow$ polarized fragmentation at Z^0 pole mostly sensitive to $\hat{\Delta\Sigma}$.
- result: Λ-polarization is about 32%
- $\hookrightarrow$ unlike DIS, $\hat{\Delta\Sigma}$ is large
- possible explanation:
  - s-fragmentation is $\approx 100\%$ polarized
  - u, d-fragmentation is completely unpolarized
    (NRQM picture!)

HERMES (G.Schnell)

- semi-inclusive $ep \longrightarrow e'\Lambda X$
- Λ polarization from parity violating decay $\Lambda \longrightarrow p\pi^-$
- q-beam composition (parton distribution + Lund): mostly u and d
- isospin $\Rightarrow \Delta D_u^\Lambda = \Delta D_d^\Lambda$
  $\hookrightarrow$ can treat as $\underline{\text{pure } u \text{ beam}}$
- HERMES result: observed Λ polarization $\boxed{P_\Lambda \approx 0}$ but probably positive
- u, d fragmentation into Λ is nearly unpolarized
- $SU(3)_{flavor}$ parameters: $\hat{D} \approx \hat{\Delta\Sigma}$
- $\hookrightarrow \quad \Delta D_u^{\Sigma^0} = \frac{1}{3}\left(\hat{\Delta\Sigma} + \hat{D}\right)$ large and positive!
- expect significant contamination from Σ^0 in
  $\Delta D_u^{``\Lambda''} = \Delta D_u^\Lambda - \frac{1}{3}\Delta D_u^{\Sigma^0}$
- $u \longrightarrow \Sigma^0 \longrightarrow \Lambda\gamma$ indistinguishable from $u \longrightarrow \Lambda$
  if γ is not detected!
- factor $-\frac{1}{3}$ from depolarization in $\Sigma^0 \longrightarrow \Lambda\gamma$.
- SU(3) $\Rightarrow \Sigma^0$ polarization positive
  $\hookrightarrow$ 'fake' Λs have $\underline{\text{negative}}$ polarization
  $\hookrightarrow$ 'true' Λs should have $P_\Lambda > 0$!

Correcting for the Σ^0

It is possible to correct the result for the production and subsequent decay of the Σ^0 in two ways:

- Fit existing data on the fragmentation of produced Λ's, which will implicitly correct for the Σ^0.
- Monte Carlo the production process, including explicit relative production rates, a model for the fragmentation process, and the unpolarized and polarized quark distributions.

I show the experimental result for the spin transfer in comparison with the predictions made in deFlorian *et al.*. They are based on fits to Λ production data in e^+e^- collider experiments.

The different scenarios, which all describe the recent results on Λ polarization ALEPH and OPAL quite well, are:

1 The naive QPM, where only the s quark is polarized in the Λ and contributes to polarized Λ production

2 The Burkardt-Jaffe model, in which u and d quarks also contribute with a negative sign

3 A rather extreme scenario, in which all the light quark flavors contribute equally to the Λ polarization.

The trend has been confirmed by a Monte Carlo simulation (Schnell) which includes spin transfers from decaying hyperons, *i.e.* the Σ^0. The resulting spin transfers are based on the spin structure of the various produced hyperons using either the naive QPM or the Burkardt–Jaffe model. Both scenarios agree with the HERMES result in the same way the scenarios 1 and 2 of deFlorian *et al.* do.

Comparison to Models

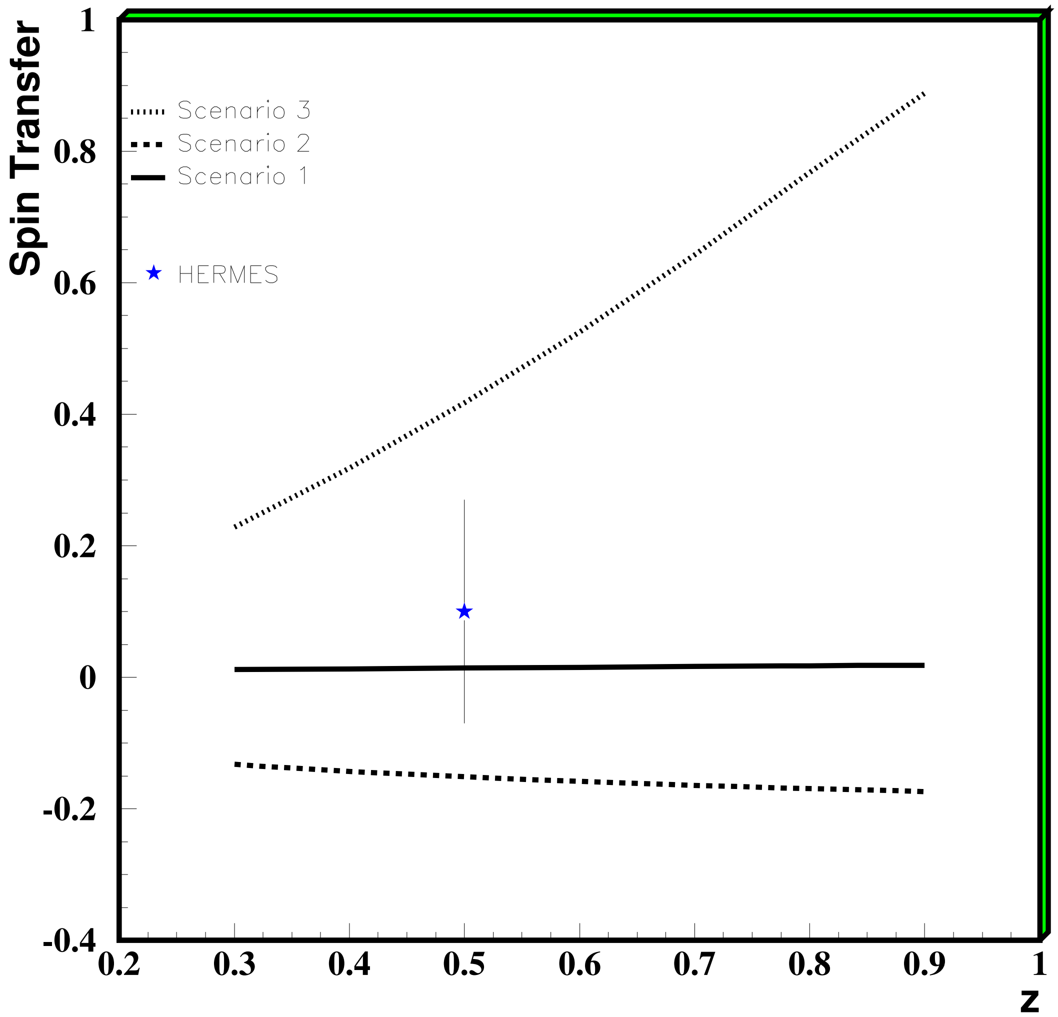

Spin transfer $D^{\Lambda}_{LL'}$ as a function of z. The curves [deFlorian *et al.*] are Q^2-evolved fits to the existing data on Λ production. Scenarios 1 and 2 use an Ansatz for the polarized fragmentation which is inspired by the spin structure of the Λ in the naive QPM (scenario 1) and the Burkardt-Jaffe SU(3) model (scenario 2). Scenario 3 assumes an flavor symmetric contribution to the Λ polarization. The data point is the preliminary HERMES result at the average z of 0.5.

At this level of measurement, polarized fragmentation looks like the naive quark parton model!

No "spin crisis" in polarized fragmentation.

But not enough data yet to make definitive statements about models.

Upgrade for improved Λ detection

In 1999, an upgrade of the HERMES detector will provide a great increase in our acceptance for Λ's. Two rings of surface–barrier detectors placed just downstream of the target area will detect pions which otherwise would have not have been in the HERMES acceptance, especially for the target fragmentation region ($x_F < 0$). This will permit much higher Λ production statistics, making it possible to map out the Λ polarization mechanism in z and x_F.

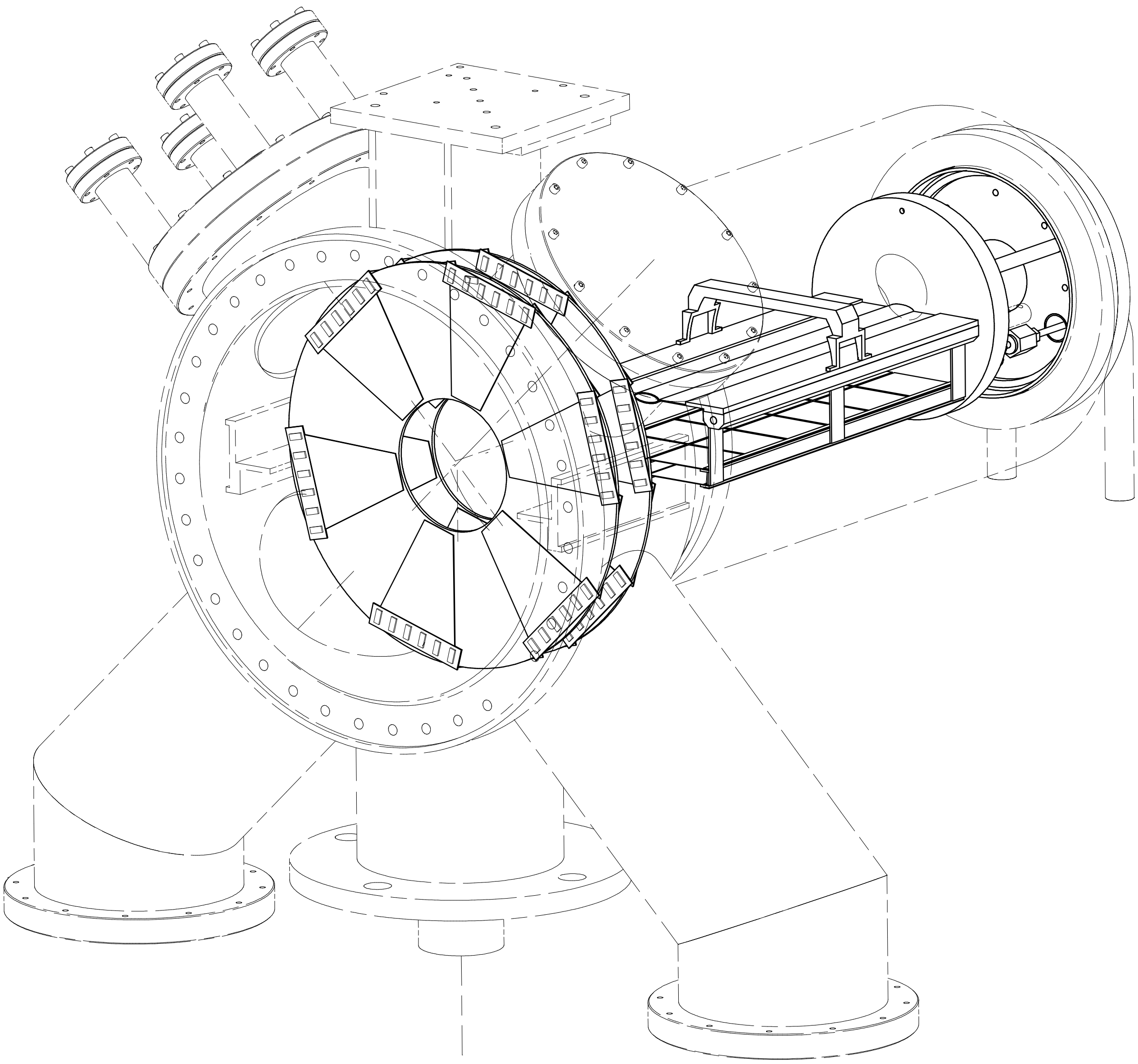

Mechanical drawing of the Lambda-wheels included in the vacuum system of the HERMES target area.

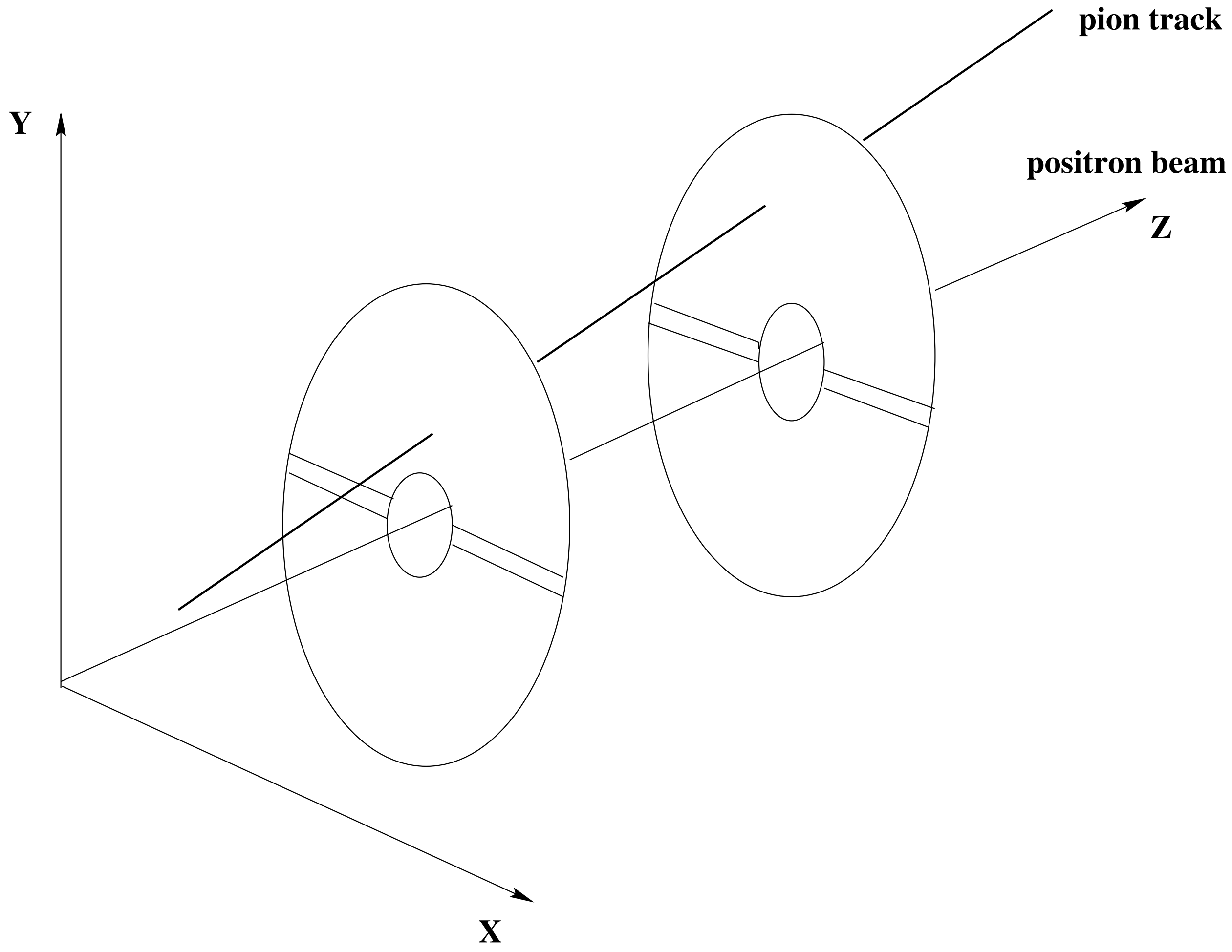

Schematic detection of a pion traversing the lambda wheels.

Reading List

1 "Beam-Induced Nuclear Depolarisation in a Gaseous Polarised Hydrogen Target," K. Ackerstaff et al. (The HERMES Collaboration), Physical Review Letters 82, 1164 (1999).

2 "Determination of the Deep Inelastic Contribution to the Generalised Gerasimov-Drell-Hearn Integral for the Proton and Neutron," K. Ackerstaff et al. (The HERMES Collaboration), Physics Letters B444, 531 (1998).

3 "Measurement of the Proton Spin Structure Function g_1^p with a Pure Hydrogen Target," A. Airapetian et al., (The HERMES Collaboration), Physics Letters B442, 484 (1998).

4 "The Flavor Asymmetry of the Light Quark Sea from Semi-inclusive Deep-inelastic Scattering," K. Ackerstaff et al. (The HERMES Collaboration), Physical Review Letters 81, 5519 (1998).

5 "The HERMES Spectrometer," K. Ackerstaff et al. (The HERMES Collaboration), Nuclear Instruments and Methods A417, 230 (1998).

6 "The HERMES polarized ^{3}He internal gas target," D. DeSchepper, L.H. Kramer, S.F. Pate, et al., Nuclear Instruments and Methods A419, 16 (1998).

7 "Measurement of the Neutron Spin Structure Function g_1^n with a Polarized ^{3}He Internal Target," K. Ackerstaff et al. (The HERMES Collaboration), Physics Letters 404B, 383 (1997).

8 "Polarized $q \to \Lambda$ Fragmentation Functions from $e^+e^- \to \Lambda + X$," M. Burkardt and R.L. Jaffe, Physical Review Letters 70, 2537 (1993).